Master's thesis

NTNU
Norwegian University of Science and Technology
Faculty of Information Technology and Electrical Engineering
Department of Engineering Cybernetics

Anders Hanssen

Strategies for reduction of low voltage PFC emissions based on pot voltage and anode current distribution signals

Master's thesis in Cybernetics and Robotics
Supervisor: Morten Hovd
June 2019

NTNU
Kunnskap for en bedre verden

Anders Hanssen

Strategies for reduction of low voltage PFC emissions based on pot voltage and anode current distribution signals

Master's thesis in Cybernetics and Robotics
Supervisor: Morten Hovd
June 2019

Norwegian University of Science and Technology
Faculty of Information Technology and Electrical Engineering
Department of Engineering Cybernetics

Summary

In the recent years, greenhouse gas emissions have received increased attention. From the aluminium industry one of the major contributions to these emissions have been from perfluorocarbon (PFC). Previously the assumption have been that emission of PFC gases only occurred during conventional anode effects, where the concentration of dissolved alumina in the electrolyte are between 0.5 - 2 wt %. Later studies have proven this assumption to be wrong. Today there are several reports which can document generation of PFC under apparently normal operating conditions. However, the underlying conditions in an electrolysis cell which contributes to these emissions are not much studied.

In this thesis the evolution of PFCs have been continuously measured by use of a Quantum cascade laser (QCL) directly mounted on the exhaust duct of a single electrolysis cell. In addition to measuring the PFCs, individual anode currents have been monitored. By using these measurements combined by the data from the process control system, insights to events contributing to increased emissions of PFC can be gained.

The main objective of this thesis is to gain insight to the production of PFCs from an electrolysis cell. This have been done by monitoring all operations that occur on a single electrolysis cell located in the production plant of Alcoa Mosjøen. This study have shown that the formation of PFCs are highly sensitive to a non-uniform anode current distribution, but also to variations in the alumina concentration in the electrolyte. Especially if the concentration of dissolved alumina in the electrolyte is in the lower range, as in the end of an underfeeding period, the production of PFC is highly sensitive to even small imbalances in anode currents.

Sammendrag

I de senere årene har klimagassutslipp fått økt oppmerksomhet. Fra aluminiumindustrien har en av de største bidragene til disse utslippene vært fra perfluorokarbon (PFK). Tidligere har det vært antatt at utslipp av PFK-gasser kun skjedde under konvensjonelle anodeeffekter, hvor konsentrasjonen av oppløst aluminiumoksid i elektrolytten er mellom 0.5-2 wt %. Senere studier har vist at denne antagelsen er feil. I dag er det flere rapporter som kan dokumentere generering av PFK under tilsynelatende normale driftsforhold. Imidlertid er de underliggende forholdene i en elektrolysecelle som bidrar til disse utslippene ikke studert mye.

I denne oppgaven har dannelsen av PFK blitt målt kontinuerlig ved bruk av en Quantum Cascade Laser (QCL) direkte montert på eksoskanalen til en enkelt elektrolysecelle. I tillegg til måling av PFK, så har individuelle anodestrømmer blitt overvåket. Ved å bruke disse målingene kombinert med data fra prosesskontrollen kan man få innsikt i hendelser som bidrar til økte utslipp av PFK.

Hovedformålet med denne oppgaven er å få innsikt i produksjonen av PFK gasser fra en elektrolysecelle. Dette har blitt gjort ved å overvåke alle operasjoner som forekommer på en enkelt elektrolysecelle som ligger i produksjonsanlegget til Alcoa Mosjøen. Denne studien har vist at dannelsen av PFK er svært følsom for en ikke-jevn anodestrømfordeling, men også for variasjoner i konsentrasjonen av aluminiumsoksid i elektrolytten. Spesielt hvis konsentrasjonen av oppløst aluminiumoksid i elektrolytten ligger i det nedre området, som i slutten av en undermatningsperiode, så er produksjonen av PFK svært følsom selv for små ubalanser i anodestrømmer.

Preface

This Master's thesis is submitted to the Norwegian University of Science and Technology (NTNU) in partial fulfillment of the requirements for the degree of MSc in Engineering Cybernetics.

This project has been done in collaboration with Alcoa, whom suggested the topic. It is an extension of a compulsory project at NTNU during the autumn of 2018. I would like to thank everyone at Alcoa Mosjøen for the opportunity to do experiments at their plant, especially Ingar Solberg for providing me with guidance and technical help during this period.

I would like to thank Thor Anders Aarhaug at SINTEF Industry for the help with the in-situ equipment used and for answering questions regarding the instrument.

I would also like to thank Prof. Morten Hovd, my supervisor at NTNU, for giving me the chance to carry out the project in collaboration with Alcoa.

Anders Hanssen, Mosjøen, June 2019

Table of Contents

List of Tables

List of Figures

Abbreviations

ACD	=	Anode-Cathode Distance
AE	=	Anode effect
CCD	=	Critical current density
CE	=	Current efficiency
EC	=	Energy consumption
FTIR	=	Fourier-transform infrared spectroscopy
GHG	=	Greenhouse gases
IUPAC	=	International Union of Pure and Applied Chemistry
LOD	=	Limit of detection
LVP-AE	=	Low voltage propagating anode effect
LV-AE	=	Low voltage anode effect
NAE	=	Non-anode effect
NP-AE	=	non-propagating anode effect
PFC	=	Perfluorocarbon
QLC	=	Quantum cascade laser
TLAS	=	Tuneable laser absorption spectroscopy

Chapter 1

Introduction

This section explains the background, motivation and objectives of the work, and uses some terms and concepts specific to the aluminium production industry. Readers unfamiliar with these terms and concepts are referred to section 2, where a more detailed description of the process and its operation can be found.

1.1 Background and motivation

Aluminium production, like any other production industry, is faced with the expectation of environmentally friendly operation. Despite significant reductions in greenhouse gas emissions from aluminum smelting over the last few decades, the industry is still a major contributor to global emissions.

Reductions in emissions have been achieved by technological improvements, but also by continuous search for new knowledge and better understanding of the smelting process. One part of the emissions in particular has received a lot of attention, the Perfluorocarbons (PFCs). Perfluorocarbons are emitted from aluminium smelters, and are highly potent greenhouse gases (GHGs) with a long lifetime in the atmosphere.

Previously there was a broad unanimity in professional circles that PFC generation only occurred during conventional anode effects (AEs) where the concentration of alumina in the electrolyte became too low, followed by a rapid increase in cell voltage. There has been a decline in PFC emissions from aluminium smelters, as seen in figure 1.1. The decline can be explained by successful implementation of techniques to reduce both duration and frequency of anode effects (Åsheim, 2017). However, recent studies have shown that PFC gases are also produced during apparently normal cell conditions. An example of these conditions could be during anode change or in the end of an underfeeding period (Batista et al., 2016). Today, the amount of PFC emissions is calculated based on the frequency of the anode effect. This indicates that the reported amount of greenhouse gases actually are higher than what is being reported. These non-anode effect (NAE) emissions can contribute significantly to the total amount of PFC emissions at a given aluminium smelter. According to reports from 13 Chinese smelters, the median contribution of NAE

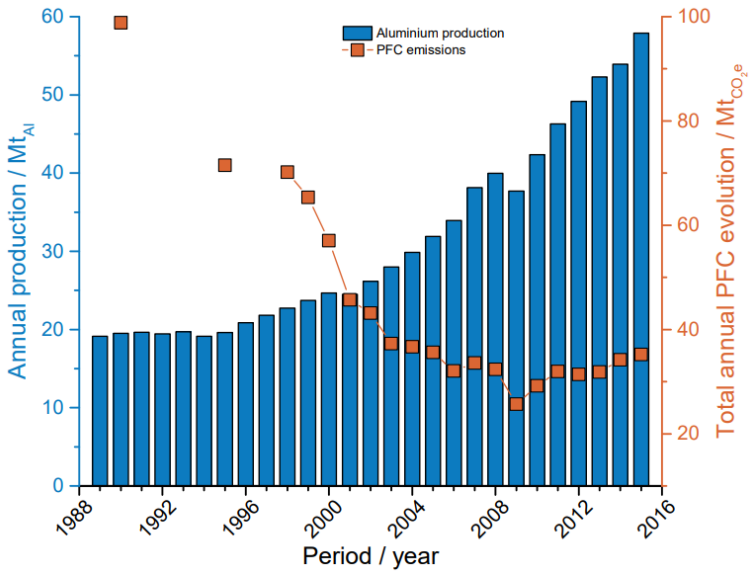

Figure 1.1: Reported PFC emissions together with annual metal production from aluminium smelters (picture courtesy of Henrik Åsheim).

emissions is 70% compared to a median contribution of 22% for 17 aluminium smelters outside China (Marks and Bayliss, 2012).

A key to understanding and preventing the production of PFC is to know which design parameters and operating conditions in the cell that contributes to the emissions. Cell design- and technology are strongly related to the probability of gas formation. It has been shown that the co-evolution of fluorocarbon species is highly sensitive to imbalances in anode current distribution, which (Rye et al., 1998) and others have connected to gradients in the alumina concentration.

Previously, there has been made little effort to gain knowledge of the development of PFCs, possibly due to the lack of instruments used to do measurements. Until today, most measurements of PFC emissions from one single industrial cell have been done by use of Fourier-transform infrared spectroscopy (FTIR). This is a reliable, but demanding process. FTIR is generally considered to be connected with high cost and require maintenance during measurement campaigns (Espinoza-Nava et al., 2016). However, the new and emerging quantum cascade laser (QCL) technology have the property to monitor pollutants in the mid-infrared range and the possibility to measure continuous, in-situ, generation of PFC. The QCL offers low maintenance and the possibility to easily mount the equipment directly to the duct on one single cell. This property gives the opportunity to gain valuable insight to which cell parameters contributing to the generation of PFC. Campaigns from a single cell can be of help to develop reliable models for estimation of fluorocarbon species from the industry. In addition, from a process aspect when the decisive conditions are known, the smelting process can be further optimized to prevent the states where the emissions are high, thus increasing production.

1.2 Objectives

The goal of this Master project is to obtain and analyze PFC measurements from a QCL on an aluminium electrolysis cell during normal operation. The cell is located in the production plant of Alcoa Mosjøen. Specifically the goal can be described by:

1. Find and analyze the conditions which are contributing to increased production of PFC.
2. Evaluate how the existing cell regulation and operational procedures contribute to PFC formation.
3. Propose a strategy to mitigate the production of PFC gases from cell control and operational procedures.

This work is a continuation of a project in the fall of 2018, when the QCL was installed and initial measurements were obtained. Roughly the same chapter about aluminium is used in the specialization project (Hanssen, 2018). However, several parts have been revised and improved for this thesis.

1.3 Outline

The structure of this thesis is set up in the following way. First, an introduction to the aluminium electrolysis process is given in chapter 2. This chapter also covers the different operations which take place in the electrolysis area and how the process control system operates. Chapter 3 describes how the different instruments used in the project were mounted and operated. It also covers which data that have been extracted and processed. In chapter 4 all the results are presented and analyzed. Finally, chapter 5 summarises the work and provides some propositions for future work.

Chapter 2

Aluminium

This chapter intends to introduce the reader to general concepts of aluminium electrolysis. If not otherwise stated, section 2.1 and 2.2 are mainly based on the work done by (Grjotheim and Kvande, 1993) and (Hestetun, 2009) and gives an introduction to development and key concepts of the Hall-Héroult process. The goal of section 2.3 is to enlighten the reader to the intuitively simple variables contributing to the process. In the last two sections abnormalities and environmental aspects of the smelting process is addressed. Topics regarding generation of PFC are mainly based on the work done by (Åsheim, 2017).

2.1 Aluminium production

Aluminium can be found almost everywhere. In anything from packing material to jet planes. Aluminium is light and strong, and new applications are continuously discovered. With about 8 % of the earth's crust, aluminium is the most abundant metallic element (Pedersen, 2018). However, because of its strong binding with oxygen it is not found in its pure form in nature, but only as combinations with other materials. The main raw material in aluminium production is aluminium oxide (Al_2O_3), often referred to as alumina. The most abundant source of alumina is bauxite. Alumina is produced from bauxite in a chemical process known as the Bayer process.

All of the industrial smelters in the world produce aluminium by the Hall-Héroult process, invented and patented in 1886 by Charles Hall in the USA and Paul Héroult in France, independently of each other. Even today, no other process have been able to measure up to this method, and it is still the only industrially viable method for production of aluminium.

2.2 The Hall-Héroult process

In the Hall-Héroult process, alumina (Al_2O_3) is dissolved in an electrolyte mainly containing molten cryolite (Na_3AlF_6). The electrolyte is often referred to as the bath. In figure 2.1 a simple sketch of an electrolysis cell is shown. The produced aluminium has a higher density than bath and is found in a liquid phase in the bottom of the cell. The carbon anodes are located on the top of the cell and they are dipped into the bath. During the electrolysis process, alumina dissolves in the bath and the oxygen is discharged onto the carbon anodes, thus forming gaseous carbon dioxide (CO_2). Based on this, the main chemical reaction during production can be written as

$$2Al_2O_{3(dissolved)} + 3C_{(anode)} \rightarrow 4Al_{(l)} + 3CO_{2(g)} \tag{2.1}$$

As we can observe from equation (2.1) the two main components in the process are alumina and carbon, and the products are aluminium and carbon dioxide. In addition to these substances the bath contains other additives like cryolite (Na_3AlF_6), aluminium fluoride (AlF_3) and calcium fluoride (CaF_2). The basic concept to remember is that while the aluminium is being produced, the anodes are consumed and have to be replaced during the electrolysis process.

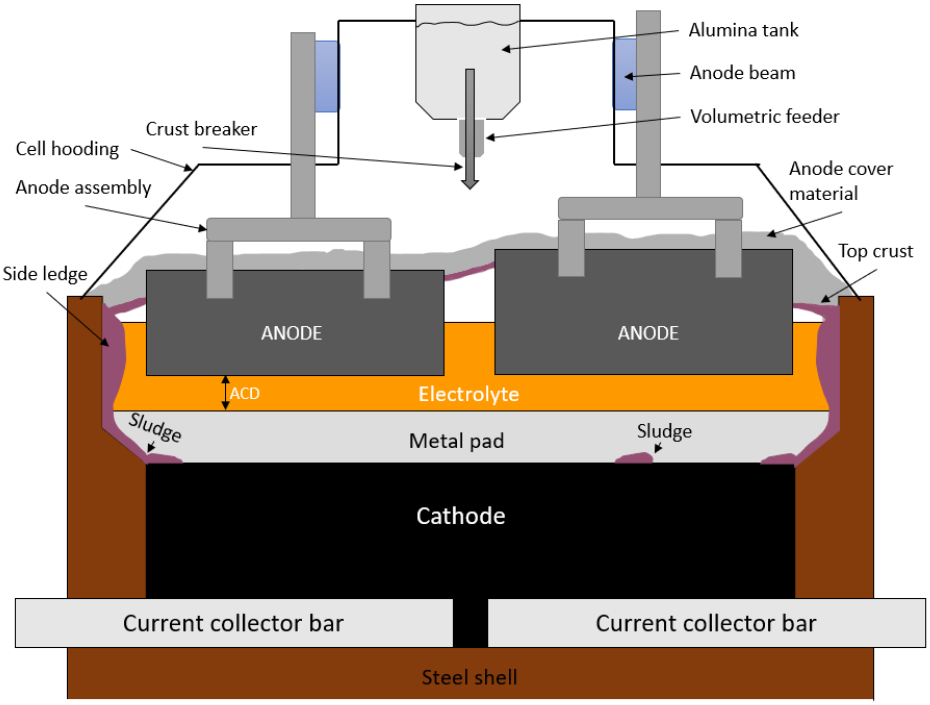

Figure 2.1: Schematic drawing of an aluminium electrolysis cell.

(a) Old anodes (picture courtesy of Alcoa Mosjøen).

(b) New anodes (picture courtesy of Alcoa Mosjøen).

2.2.1 Cell and potline design

There are two broad categories of aluminium cell design. The older Söderberg cell and the one presently preferred today, the prebake cell. The main difference between the two designs is how the carbon anodes are produced and introduced in the cells. The Söderberg cells are still used in some locations, but the design is considered somewhat outdated due to lower energy efficiency and higher emissions, and only the prebake cell design is addressed for the rest of this thesis.

The carbon anodes for a prebake electrolysis cell is produced and prebaked in a separate anode baking furnace, before the anodes can be used in the aluminium electrolysis cell, hence the name, prebake cell. This is done to ensure a higher quality of the anodes and the product produced. One benefit from producing prebaked anodes in a separate process is that the anodes does not have to be produced on site. Several smelters get their anodes shipped in from a remote location. Due to the reactions taking place in the bath, the anodes are consumed over time and they have to be replaced at a regular interval. The anodes are usually replaced when a quarter of their original length remains. In figure 2.2a - 2.2b old anodes are being replaced by a new pair of anodes by use of a crane at Alcoa Mosjøen.

Usually when the size of a cell is discussed, the physical size is not the topic, but the amperage. The electrolytic cells are connected in series and with modern design they can carry up to $600kA$ (IAI, 2018). The cells are rectangular and a hall with cells are usually called a *potline*. There are two different setups to connect the cells together in a potline, that is, side by side or end-to-end. In figure 2.3 an end-to-end configuration located at

Figure 2.3: End-to-end potline at Alcoa Mosjøen (picture courtesy of Alcoa Mosjøen).

Alcoa Mosjøen is shown and in figure 2.4 an illustration of anode and feeder position for this cell technology is shown. Anodes in the range from 1 to 9 are considered as the front side of the cell, while 10 to 18 is the backside. Not all cells are equipped with a feeder located in the center, named F3, but for the cell used in this project, figure 2.4 is representative. New potlines are usually built with a side by side configuration due to the reduced area required and enhanced magnetic field damping. Although the cells can vary in size and configuration from plant to plant, the fundamental process is still the same. The cells are connected in series. The line current enters the cell through the bus bars, distributes between the anodes and then leaves the cell through collector bars joined into the cathode carbon lining in the bottom of the cell.

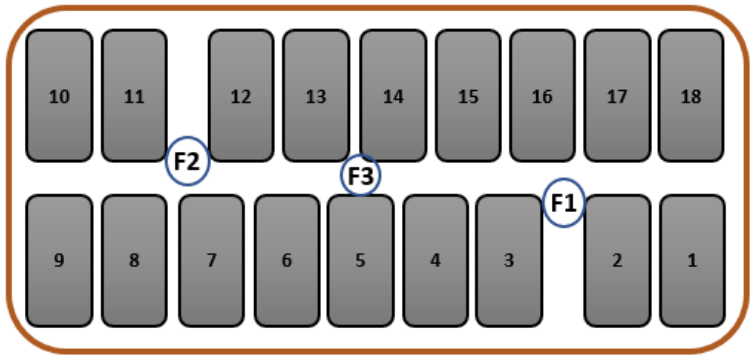

Figure 2.4: Illustration of anode and feeder positions in tested industrial cell. The duct end is to the left in the cell.

2.3 Cell operation

The day to day operation of the electrolysis cell varies. The overall goal is to keep the environment in the cell as close to given parameters as possible. Some operations are done at a regular interval. The main manual operations are sampling the electrolyte and analyzing its chemical composition, changing anodes and metal tapping. Alumina and aluminium fluoride (AlF_3) are fed to the cell automatically. Most of the operations are done with help of specialized equipment. Cranes or specialized vehicles are used to ensure safe operation when old anodes are replaced or metal is siphoned from the cell. All operations and additives to the electrolyte have some impact on the cell and they will be thoroughly described in section 2.3.2 and section 2.4.

2.3.1 Cell performance

Current efficiency and energy consumption

No industrial process is 100% efficient. For the electrolytic aluminium production process the loss of efficiency is described by the *current efficiency* (CE). CE is given as a percentage, representing the ratio of produced aluminium compared to the theoretical amount produced, see equation (2.2).

$$\text{Ratio} = \frac{\text{Actual amount produced}}{\text{Theoretical amount produced}} \cdot 100\% \tag{2.2}$$

There are several reasons that contribute to make the CE less than the theoretical amount. The main reason is when dissolved metal in the electrolyte reacts with carbon dioxide in the boundary layer of the cathode/electrolyte. This causes a reoxidation of the aluminium according to equation (2.3). This equation is called the back reaction. The best in class aluminium smelters operate with current efficiencies as high as 95-96 %. In spite of this, the average aluminium plant operates in the range of 90-94 % CE due to factors like alumina impurities or operational practices (Åsheim, 2017).

$$2Al_{(dissolved)} + 3CO_{2(g)} = Al_2O_{3(dissolved)} + 3CO_{2(g)} \tag{2.3}$$

In addition to CE there is one other parameter to describe the cell performance, *energy consumption* (EC). Energy consumption depends on both the cell voltage and current efficiency, see equation (2.4). The theoretical energy consumption is only 6.34 kWh/Kg Al at 970 °C (Grjotheim and Kvande, 1993). However, the actual EC, the ratio between actual and theoretical EC, is about 50%. Typical industrial average values are between 13-14 kWh/Kg Al with some smelters even lower. Except to losses due to CE being less than 100%, a large amount of the energy supplied to the cell is lost as heat to the surroundings.

$$\text{EC (kWh/Kg Al)} = 2.98 \cdot \frac{\text{Cell voltage}}{\text{Current efficiency}} \tag{2.4}$$

Environmental

The environmental aspects of the aluminium electrolysis process can be linked to the cell performance. The formation of undesired gases happens under conditions which lowers

the general performance of the cell. In general all the pollutants from the aluminium industry is of interest to decrease. Not only from an environmental point of view, but also from an economic view. The prebake cells are hooded to increase capturing, recovering and cleaning of the gases from the cells. In addition, the government have environmental standards which sets maximum limits of emissions per kg aluminium produced. If these limits are exceeded there may be fines or other penalties. There are also taxes that are incurred for the production of some emissions.

Generation of Perfluorocarbon

The most common PFC gases are Tetrafluoromethane (CF_4) and Hexafluoroethane (C_2F_6) which can be formed according to the two following reactions,

$$Na_3AlF_6(l) + \frac{3}{4}C(s) = 3NaF(l) + Al(l) + \frac{3}{4}CF_4(g) \tag{2.5}$$

$$Na_3AlF_6(l) + C(s) = 3NaF(l) + Al(l) + \frac{1}{2}C_2F_6(g) \tag{2.6}$$

with a standard potential, E^0, of -2.57 and -2.79 V at 960 °C, respectively. Normal production, see equation (2.1) has a standard potential of E^0 = -1.19 V and an overpotential of about 0.5 V, thus no large elevation of potential is needed for PFC generation to become thermodynamically possible (Åsheim, 2017).

Common for all the PFCs are their high global warming potentials. Their global warming potentials are about 6000 times higher than CO_2 and the increasing attention these gases have gained the last 20 years are justified. These gases can have a significant impact on the GHG emissions from one plant, and to be able to estimate the total amount of PFC emissions is of great importance.

2.3.2 Production variables

There are several variables contributing to the overall electrolysis process. In an ideal process you can calculate the theoretical amount of produced aluminium based on the input of raw materials and energy. This theoretical production rate is however hard to achieve due to all the different and dependent variables contributing to the process. If one of the variables deviate from its optimum value, this again affects other variables, and the overall performance of the cell is lowered.

Line amperage

The line amperage is the total current going through the entire potline. From a day to day perspective the line amperage is not something that is taken into consideration. Most of the time it is kept at the highest possible value for the given cell design to ensure a high production rate. However, there are scenarios when the line amperage possibly have to be reduced. This could be because of problems with the alumina feeding or in worst case a power outage. Also since the cell resistance vary independently, each cell operate at different cell voltages, this again can affect the line amperage at a small time interval if

several cells have deviating behaviour, like an anode effect, see section 2.4. This is because of the transformer being incapable of delivering enough power to keep the amperage steady at maximum level when the cells are outside their normal operating state.

Anode-cathode distance (ACD) and cell voltage drop

The average distance from the bottom of the anode to the metal pad, the anode to cathode distance, is a variable with significant contribution to the overall cell resistance. Since all the anodes are connected to the anode beam, the ACD can be adjusted as desired to achieve control of the cell resistance. By increasing the ACD, the cell resistance increases and vice versa. Since this is such an easy way to regulate the total cell resistance, adjusting the ACD is the main control action to be taken when a cell is experiencing odd behaviour. Generally, the ACD should be minimized to keep the resistance at a minimum. However, in practise there is a minimum distance that must be kept to avoid short-circuiting between the anodes and the metal surface. In addition, it has to be enough space to ensure a steady supply of dissolved alumina under the anodes, preventing locally low concentrations of alumina.

Since the total cell resistance not only varies from which cell technology being used, but also independently from cell to cell in the entire potline, there is no exact solution to what the voltage drop over a cell should be. Typical cell voltage is in the range of 4-5 V, where the modern cell designs tend to operate in the lower range of voltages.

Addition of alumina

To keep the production of aluminium going, alumina has to be added regularly to the bath. For modern aluminium potlines, so-called point-feeders are mounted into the cell and the alumina is stored in containers on the cell. This feeder technology keep the rate of alumina steady by automatically adding small amounts of alumina into the bath at a specified interval. Depending on the size of the cell, the cells are usually equipped with two to six volumetric feeders, adding a volumetrically measured amount of alumina from the containers on the cell. For the cell used in this thesis, there are three point-feeders, as illustrated in figure 2.4. Since the bath and anodes are covered with a mixture of frozen bath and fine alumina powder, a pneumatic hammer creates a hole in the crust, allowing the alumina to drop easily into the bath. Small but frequent additions are preferred due to the increased ability for the alumina to dissolve, mix, and disperse rapidly in the electrolyte (Kvande and Drabløs, 2014). If the dissolution of alumina is insufficient, the undissolved alumina will sink to the bottom of the cell forming what is called sludge. This sludge leads to increased electrical resistance, and thus increased cell voltage.

The optimal concentration of alumina in the bath is between 1.5-3.5 wt% for modern cells (Whitfield et al., 2004). The resistance in the bath is a non-linear function of alumina concentration. If the cell is operated in the higher end of alumina concentration, the problem with sludge formation would appear. On the other hand, if the concentration becomes to low, the phenomenon known as anode effect (AE) would occur. The AE is discussed more in section 2.4 and computer control of the cell in section 2.5.

Heat balance

Since the electrolyte (bath) is a highly corrosive liquid it can not be in direct contact with the side walls of the cell. To prevent this, a solid side ledge is made during startup. To maintain this protective layer, control of the superheat is crucial. Superheat is the difference between the bath temperature and the liquidus temperature. The liquidus temperature is the temperature where the frozen bath starts melting. In figure 2.5 an illustration of the side ledge is shown. With increasing superheat the side ledge start to melt, causing the heat loss to the surroundings to increase. On the other hand, if the superheat decreases, the bath will freeze and the side ledge would increase, reducing heat loss to the surroundings.

Figure 2.5: Different side ledge thickness.

Measurements of the bath temperature and acidity are done manually at a frequent interval, usually once or every other day. If there is a problem with a cell, measurements are taken more frequently. Acidity is the concentration of excess aluminium fluoride (AlF_3) relative to the cryolite composition. These two measurements give useful information about the state of the cell and are closely related to the superheat. High bath temperatures could be an indication of a too high energy input to the cell for a given bath composition, while the acidity affect the liquidus temperature of the bath. Except control of the ACD, addition of (AlF_3) is the primary input to control the heat balance. Since the alumina contains Na_2O, some of the aluminium fluoride will react with this to form cryolite, thus reducing the acidity of the bath. Also there are losses due to evaporation and release of carbon fluoride gases. To keep the concentration stable, about 20-30 kg/day have to be added to the cell. For modern cells the aluminium fluoride is added similarly as the alumina through the point-feeders.

In addition the bath and metal levels are of importance to the heat balance. Energy is required to keep the bath in liquid form and it is of importance to have the desired volume of bath and metal to ensure control of heat leaving the cell. Since the side ledge is constantly changing and evaporation of the electrolyte is present, the bath volume can change over time. If the volume is outside the boundaries, addition or removal of bath might be necessary to keep the bath temperature under control. Keeping control of the metal depth is also necessary to ensure that the amount of metal removed from the cell corresponds to the amount produced for the given period of time.

2.4 Disturbances

Generally all conditions that can bring a cell away from the optimal state can be named a disturbance. The ideal for a cell would be that none of the variables stated in the previous section varies with time, or that replacing anodes and tapping metal would be necessary. Based on this, also the routine work can be seen as a disturbance since it brings the cell outside its optimal operating state. However, there are many conditions that can be named a disturbance and in particular the anode effect is thoroughly explained due to the fairly new terminology introduced regarding this undesirable state. Cell disturbances can also be categorized by severity. For instance, crust breaking and feeding of alumina does not affect the operation sufficiently for counteractions to be performed, unless the feeding is faulty. However, after an anode change the cell often need some extra attention due to major change in behaviour. The different types of disturbances are further covered in the following sections.

Anode effect (AE)

Anode effects have been a topic of extensive study due to the quite harmful fluorocarbon gases which are being produced in this state (Wong et al., 2014). In addition, when a cell suffers from an AE no aluminium is being produced, thus causing a loss of energy. To prevent the anode effect from forming the alumina concentration have to be maintained at a desired level. If too much alumina is added, the problem of sludge formation emerges as described previously, but an insufficient amount of dissolved alumina can cause an AE to develop. The wetting of the anode deteriorates with decreasing alumina content, leading to increased gas coverage under the anode (Thonstad et al., 2000). The gas coverage under the anode act as an insulating layer, causing the resistance underneath the anode to increase. As the resistance increase, the anode current density through the anode increases. Hence, anode polarization voltage increase until the anode reaches its *critical current density* (CCD) (Tarcy and Tabereaux, 2011). When the anode(s) exceed the CCD, this can lead to a massive increase in the cell voltage. Cell voltage could possibly rise abruptly to 20-50 V without any corresponding increase in metal production (Hestetun, 2009). This type of anode effect is considered to be a *conventional* AE and was the only type known for a long time. However, since the discovery of PFC formation outside the conventional AE at what appears to be normal cell voltage (3.7 - 4.5 V) there was a need for new terminology. (Wong et al., 2014) uses the terms *low voltage propagating* anode effect (LVP-AE) and *non-propagating* anode effect (NP-AE). The LVP-AE is a result from localized AEs which rapidly propagate to a limited number of anodes with the cell still remaining below the conventional AE voltage. The last one, NP-AE is typically the one connected with the continuous formation of PFCs. This type is also named low-voltage anode effect (LV-AE). This continuous formation of PFC during what appears to be low-voltage is the one of interest for this thesis. Rapid detection and termination of the anode effect is important. The high cell voltages produce PFC, alter the bath composition, reduce current efficiency, possibly over-heating the cell and melting the side-ledge. In addition, with the high cell voltage the risk of creating an electrical arc is present.

Routine operations

There are two major manual operations that can disturb a cell from normal operation. These operations are metal tapping and anode change. In modern smelters these operations are done with help of specialized equipment, typically multi purpose cranes or specialized vehicles.

The schedule for metal tapping is site and potline dependent, but usually metal is removed from the cell once a day. How this is done is also dependent of how the potline is designed. For the location of this thesis, the metal tapping is done by crucibles attached to a crane. In figure 2.6 the metal tapping is done by use of a specialized vehicle. The metal is being siphoned into the crucible through a pipe which is lowered down into the metal pad. When the crucible is full it is transported to the cast-house. To ensure stable operation the amount of metal removed from the cell is closely monitored to balance the production. Under normal conditions the removal of metal usually goes by unnoticed, but sometimes some amount of bath can also be removed from the cell along side the metal, disturbing the heat balance in the cell. Other unwanted scenarios during removal of metal is that anodes, usually new anodes in the corner of the cells, can get stuck in the frozen side ledge, thus making it difficult to adjust to the correct ACD.

Figure 2.6: Metal tapping by use of specialized vehicle (picture courtesy of Alcoa Mosjøen).

The most critical routine operation is change of anodes. This operation usually affect the cell several hours after the operation is done. When an anode is scheduled for replacement the process starts with breaking the frozen crust surrounding the anode. This is done so the removal of the anode from the cell can be done with ease, but also so the cleaning of

the old and worn anode can be done efficiently later on. When the crust is broken and the old anode is being removed, some frozen crust and alumina which have been covering the anode will drop into the bath. Everything that falls down into the bath are grabbed by help of specialized equipment. This is done to ensure nothing is short-circuiting the new anode which is placed into the cell, or causing sludge to form in the cell. The new anode that is inserted into the cell is cold compared to the one being replaced. Due to the new anode being cold, bath freezes underneath and around the new anode. Figure 2.7 - 2.8 shows two scenarios where new anodes have been taken out of the cell after a couple of hours. The frozen bath underneath the anodes is easy to spot. Frozen bath does not conduct electricity, and thus little to no current passes through the cold anode the first couple of hours until the frozen bath melts. Since there is no electricity going through the new anodes this gives an uneven current distribution. The amount of electricity passing through the cell is still equal to before the change of anodes, but the current shifts to the other anodes in the cell since they are coupled in parallel. In addition, the uneven distribution of current in the cell can affect the flow of the electrolyte, giving gradients in the alumina concentration. Typically, dependent on the location of the replaced anodes in the cell, it takes from 12-24 hours before the new anodes are warm, and the cell operates as desired after replacing old anodes.

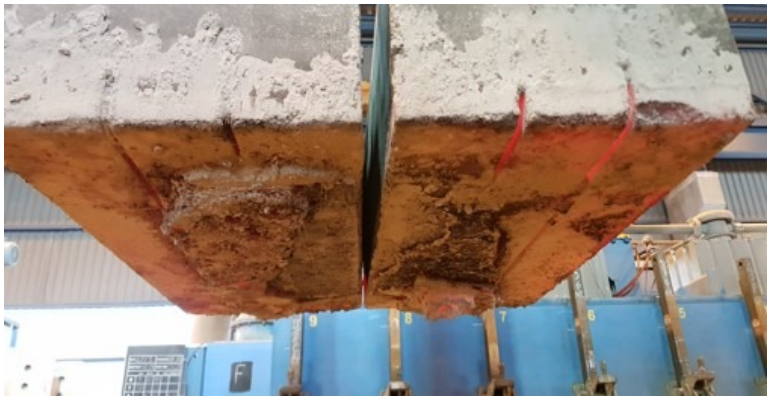

Figure 2.7: Frozen bath layer under anodes (picture courtesy of Martin Grimstad).

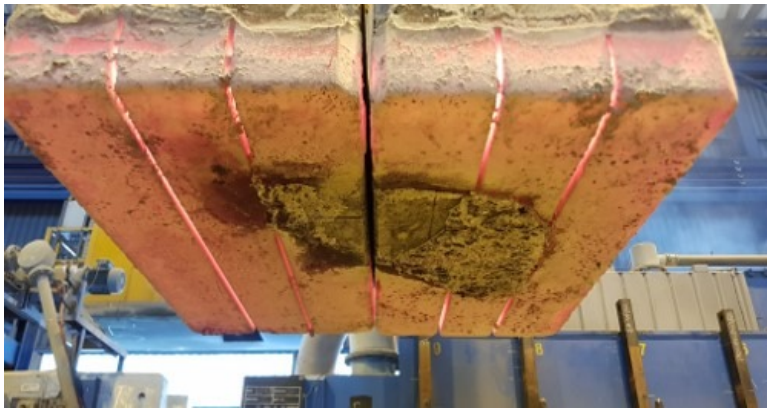

Figure 2.8: Frozen bath layer under anodes (picture courtesy of Martin Grimstad).

2.5 Cell control

How the potline was operated in the early days of mass production of aluminium is not covered in this thesis, but mainly all operations and control of the individual cells were done manually by a process operator. This was a tedious and demanding job. As new computer technology became available, it was natural to introduce this to the aluminium production. One of the main problems with introducing computer technology in a potline was the harsh atmosphere with dust and very high magnetic fields. This is however not a major problem today, and a modern potline today is full of electronic hardware and computer technology. Today each individual cell is equipped with a microcomputer that can control all automated operations. These microcomputers are also connected to an overall computer system giving the possibility to monitor and control individual cells, but also the entire potline without involving an operator. Over the years many smelters have also implemented computer systems to replace work scheduling, manual reporting and visualisation of process data. This is done not only to help the operators to do the right adjustment on a cell, but also to ensure the best possible operating conditions, hence high productivity.

For this thesis the process control is discussed based on three control objectives:

1. Resistance control.
2. Alumina feed control.
3. Handling abnormalities.

the objectives which are covered here are the ones that previous studies have correlated to increased production of PFC. The process control do cover more than the objectives stated here. In general, the overall goal of the process control system is to control variables that vary in the short-term, like ACD or bath temperature, to more slowly varying variables as acidity and bath or metal height. Each control objective specified is thoroughly discussed in the following subsections.

2.5.1 Resistance control

The electrical resistance in the cell is the fundamental key to control. Since the pot voltage changes with variations in both the line current and the cell resistance, the cell cannot be controlled by use of measured cell voltage directly. A pseudo-resistance, R_p, called cell resistance is used (Grjotheim and Kvande, 1993)

$$R_p = \frac{U - V_{ext}}{I} \tag{2.7}$$

where U is the total cell voltage drop [V], I is the line amperage [kA] and V_{ext} is the zero current intercept of U versus I for small changes in current. In theory, this minimum voltage is obtained by finding the voltage, in a volts versus amps plot. In practice, it is not necessary to find this point exactly and a small error in the value chosen has little effect on R_p. Usually V_{ext} values ranges between 1.6 and 1.8 volts. Basically, the resistance control is designed to keep each individual cell at an optimal ACD, thus balancing the need of a stable metal pad but also to ensure thermal stability in the cell.

Exactly how the resistance regulation is performed differs between companies and different technologies, but a general design approach can be described. The average cell resistance is calculated for a given time period, typical in order of minutes, and is then compared to a set target resistance, R. Around the given target resistance there is a dead band which allows a small deviation $\pm\Delta R$ around the target resistance without any need of adjusting the ACD. This control process can also be described by a simple flowchart as shown in figure 2.9.

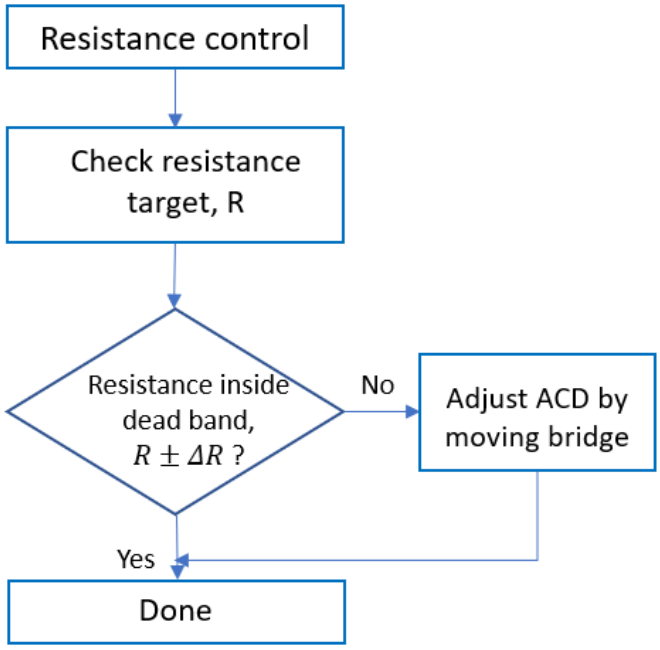

Figure 2.9: Flowchart of resistance control algorithm.

This flowchart shows the basic concept of resistance control, but in reality there are going to be several check points to go through before any adjustments are performed. In figure 2.10 a plot of resistance control from an industrial cell is shown.

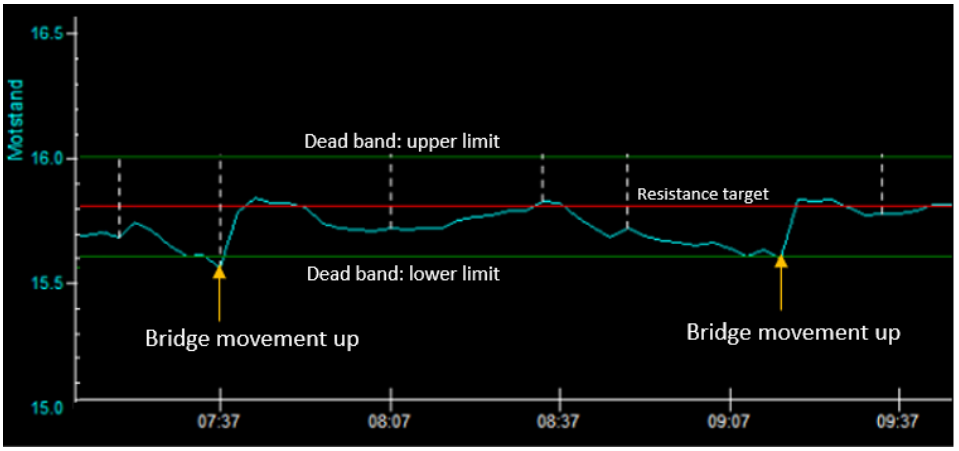

Figure 2.10: Bridge movement by resistance control.

The turquoise line is the calculated resistance. When the resistance reach the lower limit of the dead band a signal to move the bridge upwards is sent, increasing the ACD, thus increasing the resistance of the cell.

2.5.2 Alumina feed control

Keeping control of the alumina concentration in a cell is a key feature to ensure high current efficiency in the cell. Before the use of computers to control the addition of alumina it was normal to schedule an anode effect to occur on a cell at a regular interval. This was done to ensure that the concentration of alumina in the electrolyte did not become too high, resulting in sludge formation in the cell. If the electrolyte becomes saturated with alumina, undissolved alumina starts forming a sludge which have a higher density than both the electrolyte and molten aluminium. Eventually this sludge will deposit on the bottom of the cell as seen in figure 2.1 and cause stability problems. On the other hand, if the alumina concentration gets too low, an anode effect occurs as described in section 2.4.

Today, with use of computer control it is possible to achieve a much tighter control of the alumina concentration in the electrolyte. An alumina feed control algorithm determine when the cell point feeders will operate and drop a new batch of alumina down in the electrolyte. By use of this method it is possible to keep the alumina concentration in a desired range, and the cells can operate for a long period of time without any AEs or indications of sludge formation. The most common problem related to the feed control system is not connected to the feed control algorithm, but to mechanical faulty point feeders.

Since there are currently no technology to measure the composition of the electrolyte continuously, the alumina feed control algorithm have to gather information of the alumina concentration from a different relationship in the electrolyte. There is a relationship between the total cell resistance and the electrolyte alumina concentration. This relationship also varies with the ACD according to figure 2.11.

The feed control algorithm is utilizing this relationship frequently to infer the alumina concentration. From figure 2.11 it can also be noticed that the shape of the curve does

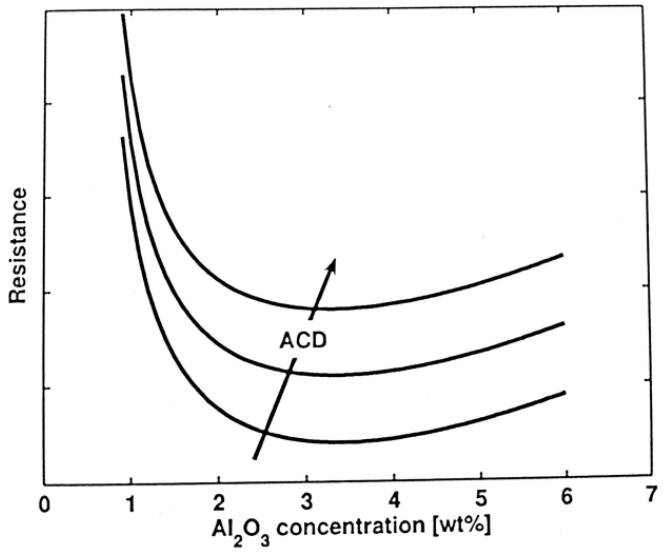

Figure 2.11: Variation in total cell resistance with alumina concentration and anode-cathode distance (Hestetun, 2009).

not change, it only translates in space. In the ideal case the alumina concentration would be at a fixed rate at all time, however in practice this is not possible and some variation is necessary since the curve cannot be used directly for control purposes. The basic idea of the alumina feed control algorithm is to look for a change in pseudo-resistance, or a change in the slope of the pseudo-resistance versus alumina concentration curve, while the alumina concentration in the cell is deliberately changed in a specified direction. This change of alumina concentration is obtained by altering between an overfeed- and underfeeding period. By feeding the cell at a constant feed rate that is lower than the theoretical consumption of alumina, the pseudo-resistance can be expected to decrease, as we can observe in figure 2.12. It can easily be observed that as the feed cycle enters an underfeeding cycle, the resistance slope start to increase. When the resistance slope reaches a specified limit, the feed cycle changes to an overfeed (marked with red circles) to prevent the concentration of alumina to become too low in the electrolyte.

How the alumina feed algorithm terminates the different feed cycles differs, but its natural to set the termination limit so that the cell does not become starved of alumina, with the risk of an AE to occur. Exactly how the termination limits are set is in the scope of this thesis and will be further discussed later with respect to production of PFC.

2.5.3 Controlling abnormalities

Noise control

For the alumina feed control to operate as tight as desired, the cell have to be stable. If a cell is unstable it usually has *noise*. Noise is a term used to describe the variability of

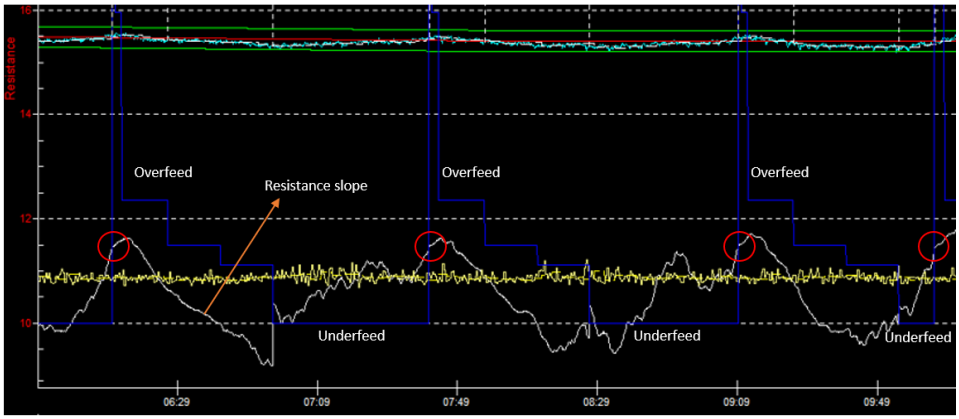

Figure 2.12: Variations in resistance slope and alumina feed cycle.

the cells resistance signal over a relative short period of time. If the noise is high, the alumina feed control is going to have trouble calculating the correct slope, with the result of inaccurate alumina feeding.

The goal of the noise control is to make the cell operate at the minimum ACD required while the stability of the cell is maintained. This allows the CE to be maximized by minimizing the back reaction as described in section 2.3.1. The noise control only affects the instability which is caused by horizontal currents in the metal pad. Horizontal currents upsets the metal pad stability. Generally, noise control simply works by increasing the ACD by adding temporary resistance modifiers if the noise is over a maximum limit. The increased ACD stabilizes the metal pad by decreasing the horizontal currents in the metal pad. When the cell noise have been under the maximum limit for a given time, the temporary resistance modifier is removed. In figure 2.12 the yellow curve represents the noise for a stable cell.

Variations in cell resistance can also be caused by many other problems in the cell. Pieces of carbon at the bottom of the cell can short circuit anodes, wrong ACD when old anodes are replaced, spikes underneath the anodes, or faulty anodes are some events that can cause short term variations in the cell resistance. Temporary resistance modifiers are going to be added for these events too, probably removing the noise. However, when the temporary resistance modifier is removed from the cell, the noise is going to appear again. The noise control is going to add and remove a resistance modifier until an operator finds and remove the problem causing the noise.

Anode effect termination

The ability to reduce duration and frequency of an AE is important. Since an AE is bad for production, the AE control usually has precedence over any other control logic. Once an AE is detected by the process control, a procedure immediately starts to terminate it. There are different techniques to terminate an AE. Generally, the isolating gas layer under the anodes must be removed by disturbing the electrolyte, and alumina must be rapidly added

to replenish the depleted alumina concentration in the electrolyte. Modern smelters have automatic procedures to suppress and terminate an AE. The common technique is lowering the bridge to short circuit the anodes to the metal pad while increasing the alumina feed rate to the cell. If the process control fails to terminate an AE, it is necessary to manually insert a wooden stick underneath the anodes to disturb the electrolyte and remove the gas layer. Some smelters blow air under the anodes to get the same effect.

Chapter 3

Measurement data

This chapter gives an overview of all the equipment and process data required. Section 3.1 will cover the different equipment used, while section 3.2 covers the extracted data from the process database.

3.1 Equipment setup and measurements

3.1.1 Anode current measurements

Each of the anode rods on the prebake cells at Alcoa Mosjøen is connected to the bus bar by an individual flexible connection. By measuring the ohmic voltage drop across the flexible connection, the current passing through each individual anode can easily be monitored. To utilize this information the cells are equipped with a display with LED bars. Each column of LED bars represent the current going through each individual anode (Rye et al., 1998). If one or several anodes has irregular current consumption, this will appear on the process data which the operators use to monitor each cell. If a problem occurs on a cell, the cell display can give the operators valuable information regarding the state of the cell. For example, if one of the LED bars is peaking, this is an indication of an anode with a problem, causing the cell noise to increase.

The individual anode current readings are not stored automatically for later use. To utilize the anode current data available, a multi-channel logger (from DATAQ Instruments) is connected to the cell display to record the different voltage signals going to the LED bars. The multi-channel logger is connected to a local internet by wireless setup so the software (WinDaq) can be accessed remotely. See figure 3.1 for an overview of the software used for individual anode current logging.

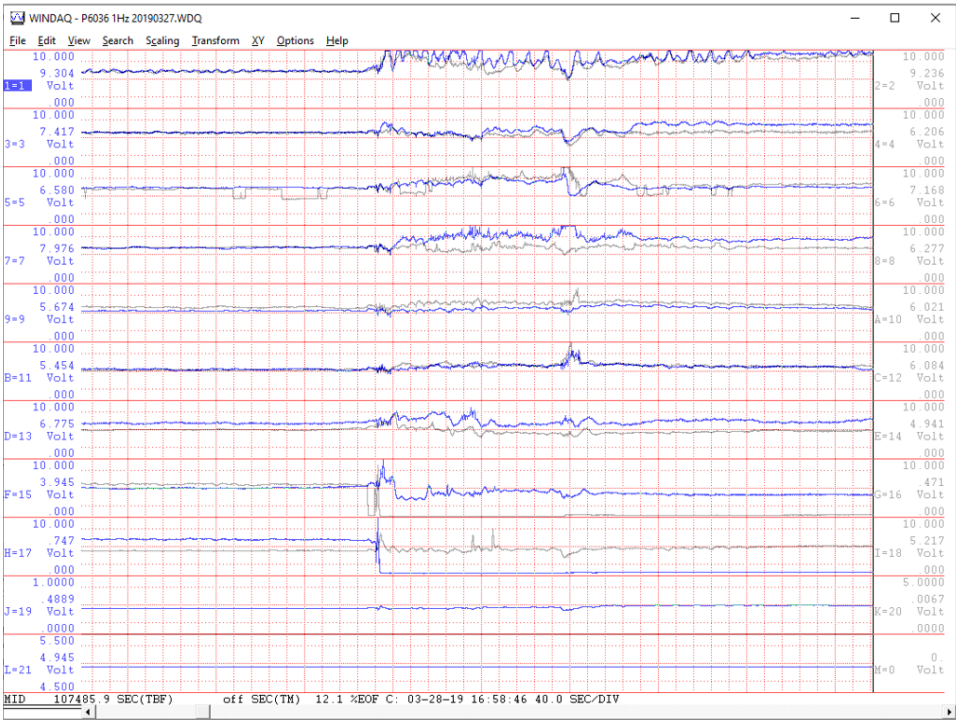

Figure 3.1: Overview of WinDaq software.

The time series from 1-18 are equivalent to the voltage recorded over anode 1-18. In addition to recording the anode current distribution, the cell voltage is also recorded with the same frequency. The cell voltage is divided by 10 and is located in the time series named 19. The rest of the time series can be ignored. In the software, sampling time can be specified at startup. For this setup the data can be sampled down to 1 sec.

3.1.2 PFC measurements

The key instrument used to monitor PFC emissions from an electrolysis cell in this project is the Quantum cascade laser. The QCL is a LaserGas™ Q CF4 delivered by Neo Monitors and its based on tuneable laser absorption spectroscopy (TLAS). The instrument consists of a transmitter and a receiver unit to measure the average gas concentration along the line-of-sight path (NeoMonitors, 2018). The measuring principle will not be dealt with here, for details see the manual of the QCL (NeoMonitors, 2018). In figure 3.2 an overview of the instrument is illustrated.

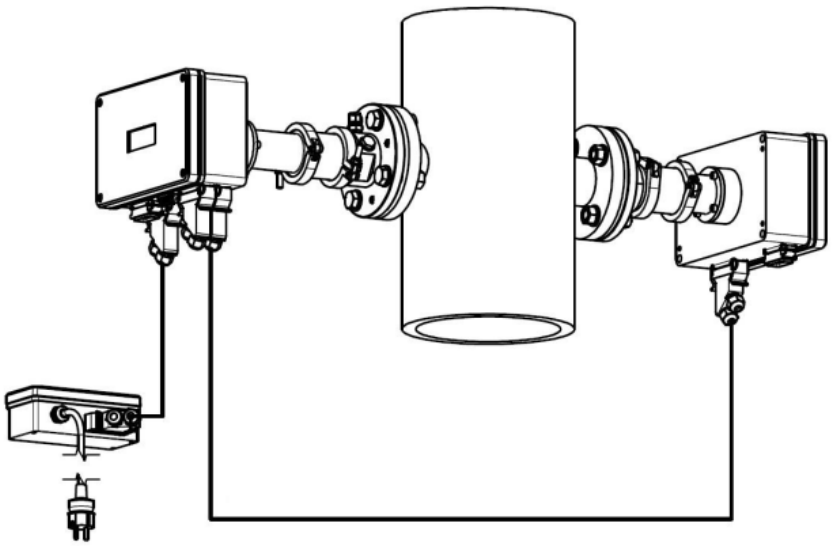

Figure 3.2: General view of LaserGas™ Q CF4 (NeoMonitors, 2018).

Before use, the instrument was calibrated at SINTEF. The calibration showed that the measured value of CF_4 is around 1.4 times higher than the true value, see figure 3.3. The correlation is linear and can be corrected for (Aarhaug, 2019). According to IUPAC, the signal to noise ratio should be minimum 3 standard deviations. This gives a limit of detection (LOD) of 35 ppb for the blank measurement, see figure 3.4. In this experimental set up, the line-of-sight path for the QCL is equal to the duct diameter, which is 0.4 m. This corresponds to a LOD of 26 ppb for this set up, assuming linear correlation between path length and LOD.

The portable size of the instrument is what makes this instrument ideal for this scope of work. The size is what make it possible to mount the QCL directly to the exhaust duct of a single aluminium electrolysis cell so that continuous measurements of CF_4 can be recorded (Aarhaug et al., 2018). The location of the instrument is carefully thought through. Except from pressurized air and power, the instrument needs a minimum light path between the laser head and detector. In addition, one must remember that the potline contains a lot of heavy equipment and operators, which should not be disturbed by the instrument. In figure 3.5a and 3.5b the QCL fully assembled to the duct is shown.

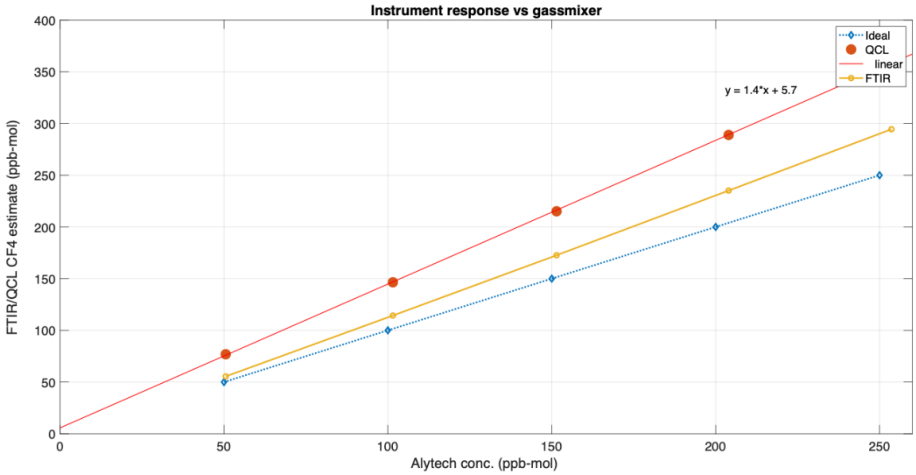

Figure 3.3: Validation of the LaserGas™ Q CF4 (picture courtesy of Thor A. Aarhaug).

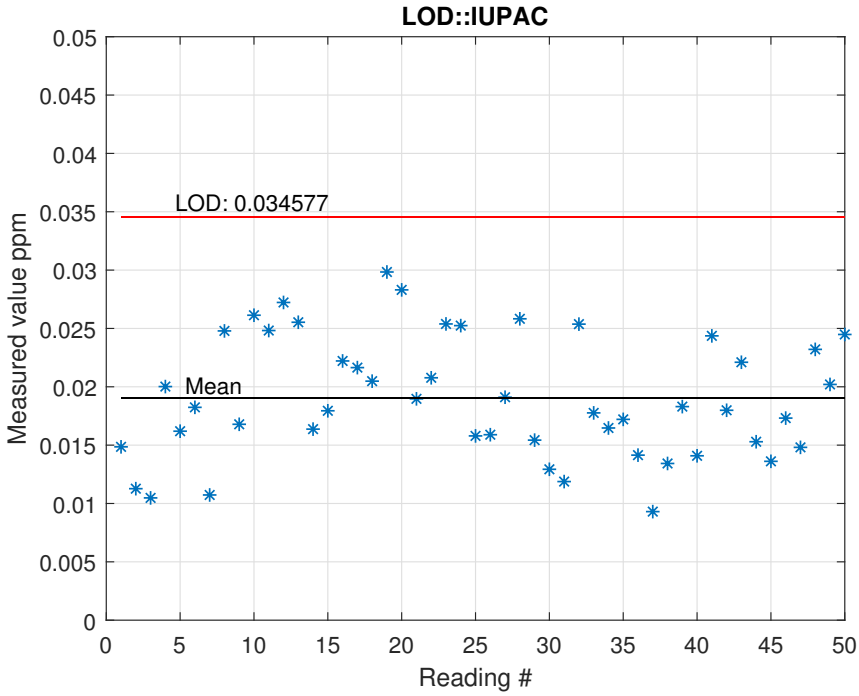

Figure 3.4: LOD of the LaserGas™ Q CF4 (picture courtesy of Thor A. Aarhaug).

(a) LaserGas™ Q CF4 transmitter unit.

(b) LaserGas™ Q CF4 detector unit.

Before it was possible to mount any of the instruments, flanges had to be welded to the duct. The transmitter and detector were mounted directly to the flanges. It is important that the transmitter and detector unit are mounted diametrically opposite each other. The required transmission was obtained by adjusting locking screws between the flanges on the duct and flanges holding the instrument. Pressurized air was connected to the instrument flanges to keep the instrument windows clear from particles and to cool the transmitter unit. Nonetheless, in some periods the instrument required some maintenance. In figure 3.6 the optical window of the detector unit is covered in alumina from the cell and had to be cleaned to obtain good transmission.

In the QCL configuration software the light path was set equal to 0.4 m and the temperature was set to 125 °C. The temperature measurement of the gas was done by use of a thermocouple. Since these two parameters were fixed, this is a possible source of concentration offset for the QCL. The ideal would have been to feed the instrument with temperature- and pressure values directly from transducers connected to the instrument so the software could calculate the concentration based on these parameters directly (Aarhaug et al., 2018). The initial sampling time was set to 1 sec, but was increased to 3 sec later on. The QCL was connected to a local internet by a wireless setup so the QCL software and log files could be accessed remotely, see figure 3.7 for an overview of the QCL configuration software.

Figure 3.6: Detector optical window before cleaning.

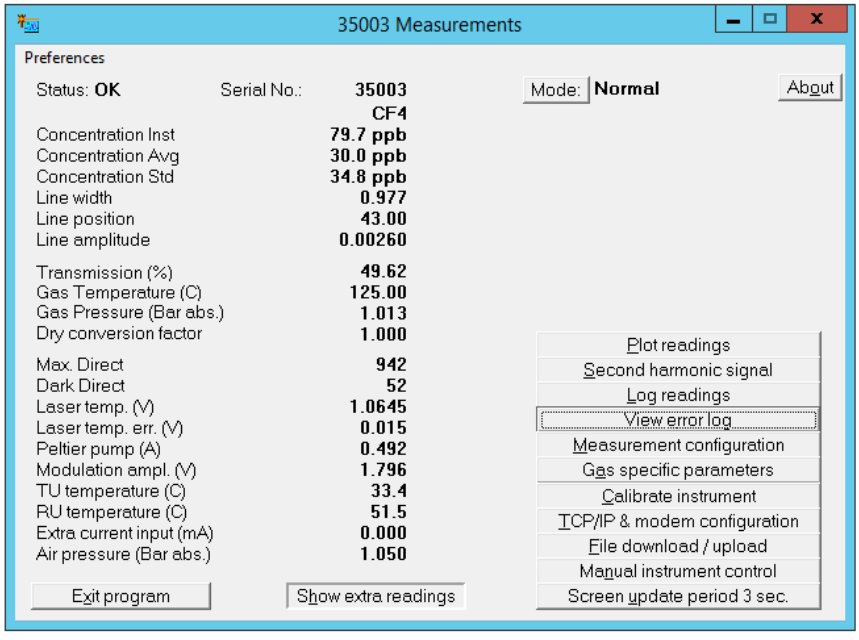

Figure 3.7: LaserGas™ measurement menu (by Neo Monitors).

3.2 Cell process data

All the data from the potline control system is stored in a process database. Not all data stored is of importance for this project. The process data of interest for this scope of work in addition to concentration of CF_4 and individual anode currents are listed in table 3.1. This process data is usually what is used by operators to check the status of a cell. An experienced operator can use these measurements to see if, for example, a cell is saturated with alumina or other preventive actions are necessary.

Table 3.1: Extracted process data.

Process data
Resistance
Resistance target
Resistance modifier
Cell voltage
Noise
Resistance slope
Resistance slope target
Feed interval [sec]
Feed rate [%]
Anode imbalance [%]

It is important to notice that some of the data in table 3.1 are set points (target) to the process control system, and not measured values. In addition, the actual alumina feed rate can be affected by varying batch sizes, both with time and from feeder to feeder (Hestetun, 2009). Other scenarios like insufficient crust breaking, or changing ACD can also affect the actual feed rate if lumps of alumina falls into the electrolyte.

3.2.1 Data processing

Some processing of the raw data had to be performed. The CF_4 measurements from the QCL contained a lot of high frequency variation that is not directly related to any dynamics in the cell behaviour. These measurements were simply smoothed by taking the moving average over a window with length $N = 100$. See figure 3.8 for an example of the smoothing technique compared to the original data.

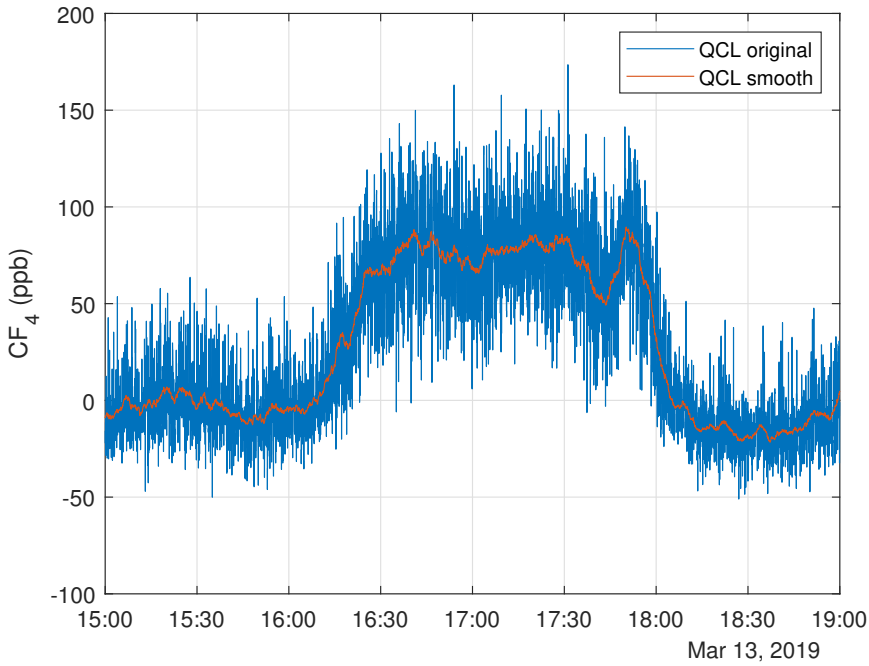

Figure 3.8: Smoothed QCL response.

All the data recorded by the different instruments and data from the process database operates with different time vectors and sampling intervals. For example, the QCL creates a new log file at midnight and the timestamp of each measurement is given in seconds since the creation of the log file. Due to this, MATLAB scripts and functions were developed to extract data and convert time to the correct format from the different log files and databases.

Chapter 4

Experimental work and results from Alcoa potroom

Since aluminum production is a process that takes place around the clock there is a large amount of measurements available and data to analyze. This section describes the measurement series that have been recorded and the conditions under which they were recorded. The type of measurement series can be divided into two groups:

- Measurement series recorded under normal operation. For example, anode change, metal tapping or normal alumina feeding.
- Measurement series recorded during experiments where the cell is exposed to conditions that represent faulty equipment or otherwise represent undesirable operating conditions.

Section 4.1 covers the different events and experiments which has been completed throughout this period to collect data. The main findings will be presented in section 4.3 to section 4.5. Some of the events are quite similar and not all of the gathered data will be discussed in this thesis. For readers unfamiliar with operating an electrolysis cell, the results can be tough to grasp. To prepare the reader, some concepts are repeated in section 4.2. A description of the different plots used to present the results is also given in this section.

As an introduction to the results, the case of a cell operating without any problems is presented. That is, the cell have an uniform anode current distribution and normal alumina feeding, see section 4.3. The rest of the results are presented and analyzed by the same grouping as in table 4.1. It should be noted that the results are not analyzed with the aim of quantifying the total amount of PFC emissions, but rather to find the the underlying causes of elevated CF_4 concentrations.

4.1 Events and experimental work

The goal of the experimental work have been to introduce the monitored cell to various events to see how the production of PFC from the cell is affected. Some events have previously been correlated to co-evolution of PFC emissions by use of FTIR. However, the online monitoring provided by the QCL gives an opportunity to easily monitor and correlate emissions with the process (Aarhaug, 2019). The different type of events have been sectioned into two groups,

1. Events that can cause non-uniform anode current distribution.
2. Different alumina feed settings.

In table 4.1 an overview of the different events and planned cell operations are listed by the groups mentioned. Each type of event is only listed once, but some events are performed several times to collect more data. A detailed description of the different events is given in the problem description of section 4.3 and section 4.5

Table 4.1: Overview of all events and data series.

Group	Events
1	Anode change
1	Anode problem/imbalance
1	Preheated anodes
2	Normal alumina feed cycle
2	Aggressive underfeed of alumina

4.2 Basic concepts and description of plots

A way to distinguish a stable cell and an unstable cell is by measuring the level of *noise*. Noise is a term used to describe the variability of the cells resistance signal over a relative short period of time. For more details about noise and what causes noise, see section 2.5.3.

The alumina concentration is obtained by altering between an overfeed- and underfeeding period. In this thesis, normal feed rate is 100 %. Periods under and above 100 % are considered as underfeed and overfeed, respectively. This is done deliberately to identify changes in the slope of the pseudo-resistance versus alumina concentration curve, see section 2.5.2 for details. If the variance in the cells resistance signal is large, the *noise is high*. High noise causes a problem for the alumina control system since its difficult to get a reliable measure of change in the calculated slope.

For a stable cell, the anode current distribution is *uniform* across all of the anodes. If the anode current distribution is *non-uniform*, this is a sign of one or several anodes using more current. It does not necessary have to be a steady over-consumption. Often the currents fluctuate between high and small values, with the result of variability in the cells resistance signal, causing increased measurements of cell noise. In the results the anode current

distribution is presented two ways. One time series and one with use of box plots. The time series is good for giving information about when an event occur. The event of an anode change can be seen by one of the curves in the time series, representing each individual anode, dropping towards zero. However, the time series does not provide an easy way to compare each anode to each other. This is where the boxplot comes to use. The boxplot is used to display the distribution of the individual anode currents prior to and after an event. On each box, the central mark indicates the median anode current, and the bottom and top edges of the blue box indicate the 25th and 75th percentiles, respectively. The whiskers extend to the extreme measurements, and all measurements over this is considered as an outlier, plotted individually with the red + symbol. The outliers in this case gives information about the fluctuations in the anode currents, since these are extreme values compared to the median current. In addition, with the box plots it is easy to see how each individual anode current measurement is contributing to the cell noise. Notice that the anode position in the box plots is equal to the one presented in figure 2.4. This is done to easily see how the currents shifts between anodes adjacent or opposite of each other.

4.3 Analysis of PFC emissions during uniform anode current distribution

4.3.1 Problem description

To establish a baseline for comparison of PFC production, it is necessary to have PFC production data for a cell without operational problems. When a cell is operating with no operational problems there should not be any PFC emissions. This is due to sufficient transport of alumina in the electrolyte and an uniform anode current distribution. For an uniform current distribution it can be assumed that all of the anodes operates under the CCD.

4.3.2 Results and discussion

As seen in figure 4.1 the anode current distribution is not entirely uniform, but the alumina feed rate was operating normally, cycling between under- and overfeed periods. Anode #18 was replaced about 18 hours prior to this window and is starting to pick up current. However, there are no major peaks of CF_4 to be taken into consideration for this period of time. The spike in the CF_4 measurements at 17:30 is from cleaning the optical windows on the instrument and should not be considered. Based on the data presented in this case, it is possible that there is some background PFC emissions for an uniform anode current distribution with normal alumina feeding to the cell. However, these PFC emissions is small in magnitude and below the LOD of the QCL in this case.

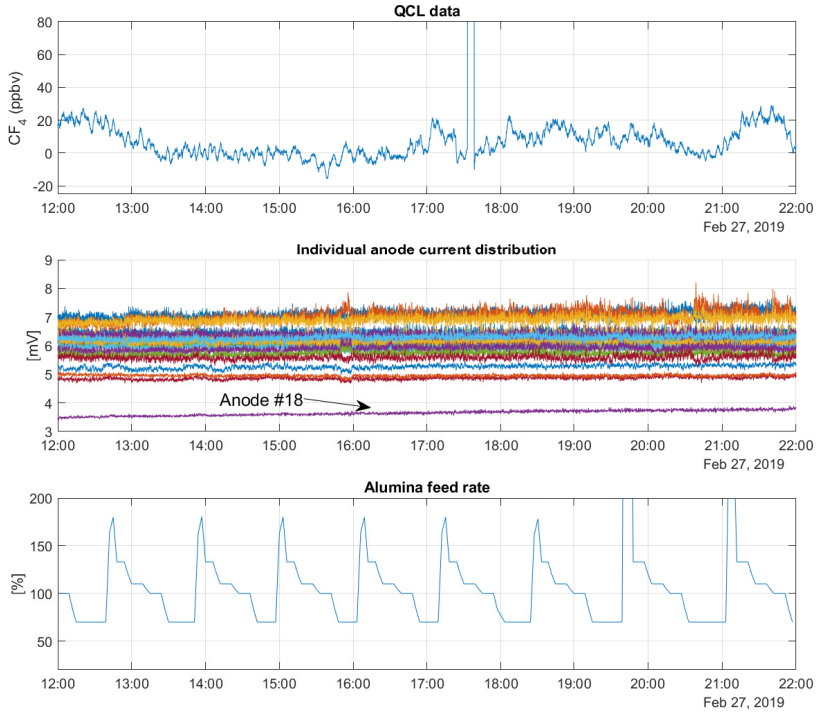

Figure 4.1: No operational problems during a 10 hour window.

4.4 Analysis of PFC emissions during non-uniform anode current distribution

4.4.1 Anode change

Problem description

As mentioned in section 2 the currents through the individual anodes adds up to the total potline amperage. If the current through some of the anodes changes, like during replacement of old anodes, this gives an uneven current distribution among the rest of the anodes in the cell. One cannot accurately predict how the current redistributes among the anodes. More current will flow where there is less resistance. Anodes adjacent to the ones being replaced usually take up a higher current load after the new and cold anode(s) is placed in the cell, with the risk of exceeding the CCD. Events related to a non-uniform current distribution happens regularly. This is not only caused by anode change. Spikes underneath the anodes can cause shortenings between the anode and metal pad, with the result of oscillating currents through the anode. Since the QCL offers continuous monitoring of PFC, there are many events and measurements for the time period of this thesis to collect. For this smelter, anode change is planned with 2-4 days in intervals. The operators have not been made aware that measurements are taking place. This is to ensure that all operations are done like normally. In addition to the results presented here, tables with calculated change in mean- and peak currents for each anode can be found in appendix A.

Results and discussion

Case 1

For this case there is nothing special that occurs. In figure 4.2 it can be observed that leading up to the anode change at 15:30 the cell has no operational problems. Around 14:45 there is an increase in the concentration of CF_4. However, the increase cannot be linked to any other operational data in this case. The anode current distribution after the anode change does not change much. In the boxplots in figure 4.3 the fluctuation in currents after the anode change is noticeable. However, from table 1 in the appendix the highest mean increase in anode currents is found to be 29% on the anode in position 6. At 17:00 the concentration of CF_4 drops with the change from underfeeding to overfeeding of alumina to the cell. This could possibly be an indication of a too low concentration of alumina during this period after the anode change.

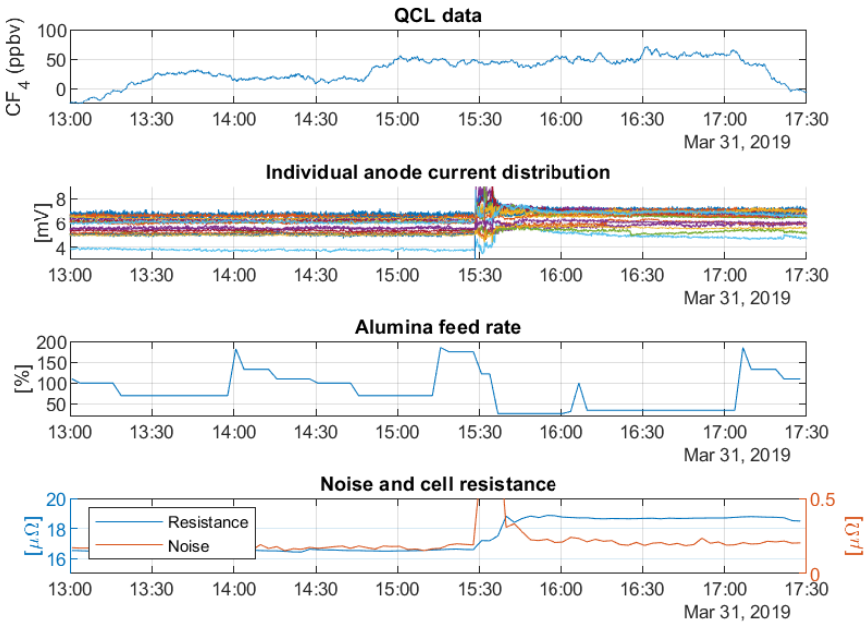

Figure 4.2: Case 1: at 15:30 the anodes in position 14-15 are being replaced.

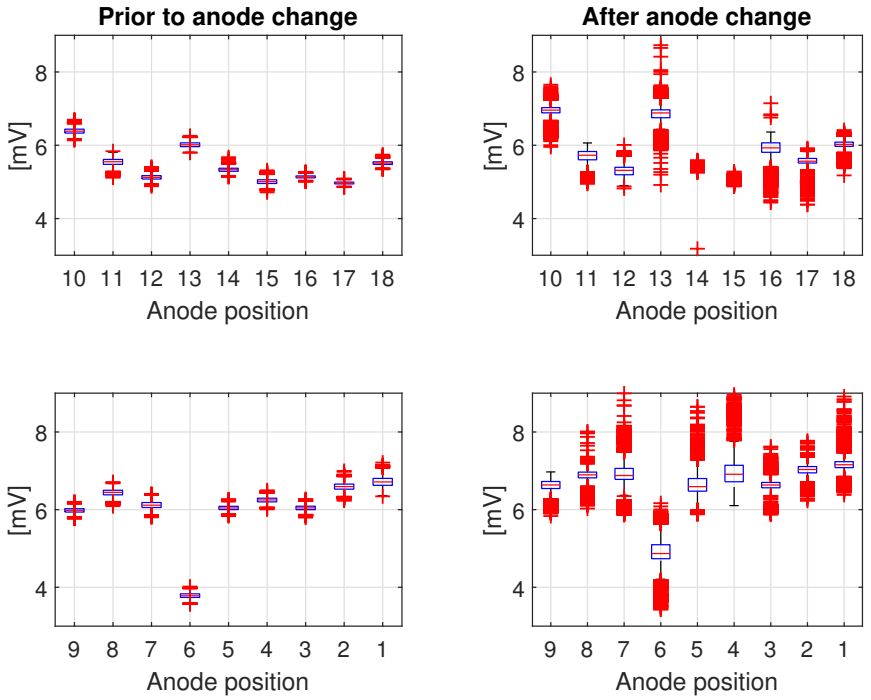

Figure 4.3: Case 1: Boxplots of individual anode currents over the period depicted in figure 4.2. Boxplots prior to anode change is from 13:00-15:30. Boxplots after anode change is from 15:30-17:30.

Case 2

In figure 4.4 the anode change can be observed at 15:45. At the same time the concentration of CF_4 starts to increase. In this case, the distribution of current through anodes opposite of those being replaced is noticeable. The anodes in position 12-13 is the one being replaced. In figure 4.5 it is easy to observe the rise in current through the anodes opposite of anode 12-13. From table 2 in the appendix, the peak currents through anode 4,5 and 7 ranges from 88 to 98% compared to the mean currents prior to the anode change. At 16:50 it can be observed from figure 4.4 that the concentration of CF_4 drops with the change from underfeeding to overfeeding of alumina to the cell. This could possibly be an indication of a too low concentration of alumina during this period after the anode change.

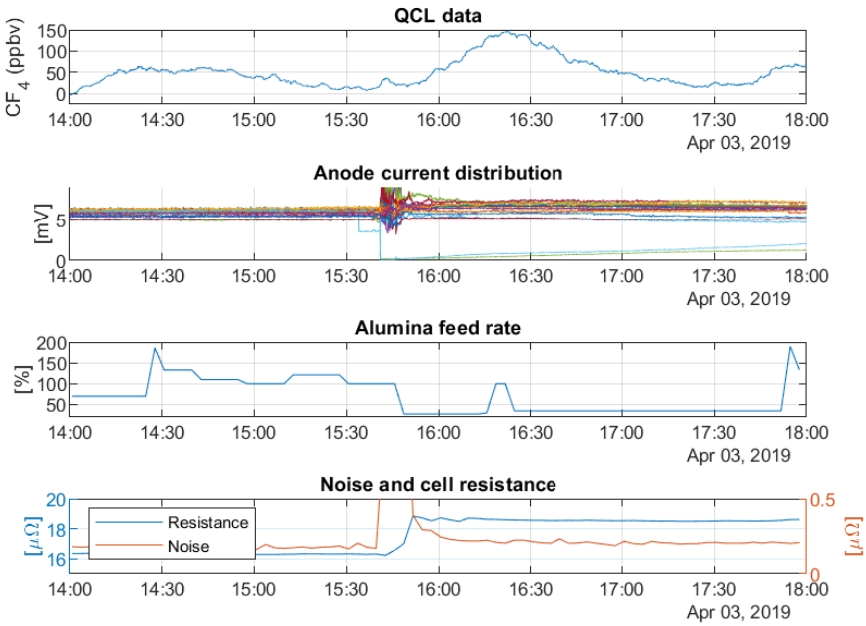

Figure 4.4: Case 2: at 15:45 the anodes in position 14-15 are being replaced.

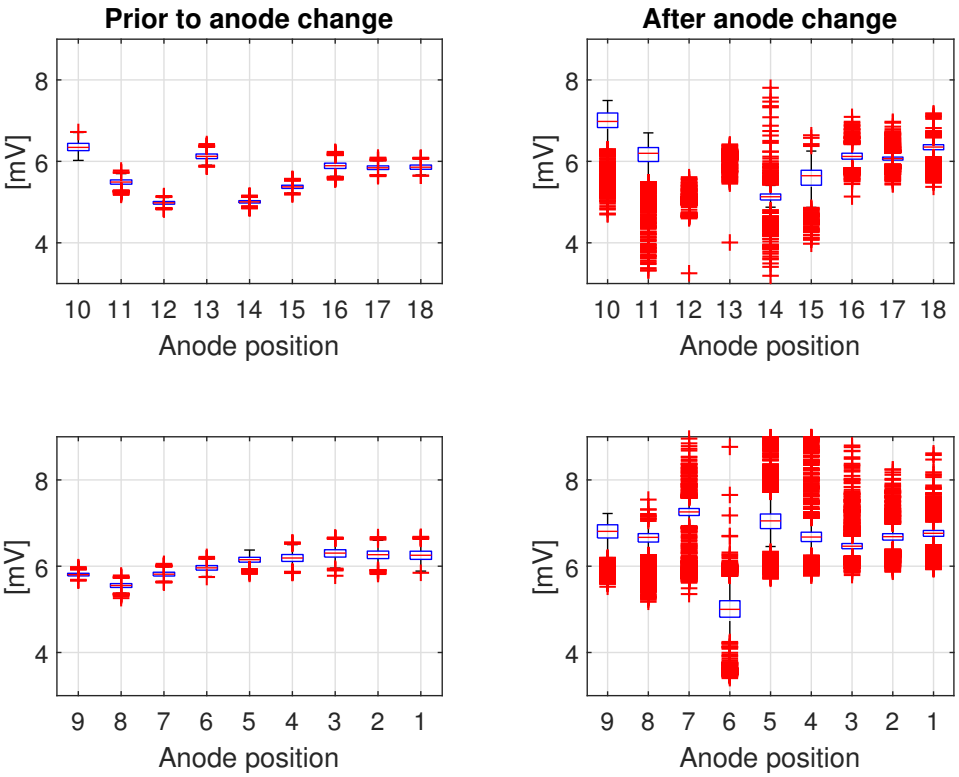

Figure 4.5: Case 2: Boxplots of individual anode currents over the period depicted in figure 4.4. Boxplots prior to anode change is from 14:00-15:45. Boxplots after anode change is from 15:45-18:00.

Case 3

In figure 4.6 the start of the anode change can be observed around 15:00. The anodes in position 10-11 is the one being replaced. Note that the data for the anode in position 12 are omitted due to a faulty sensor. At the same time as the anode change starts, the concentration of CF_4 starts to increase. In figure 4.7 high peak currents can be observed after the anode change. From table 3 in the appendix it can be observed that there are several anodes with peak currents in the range of 91% - 111% compared to the mean currents prior to the anode change. In addition, the anode in position 9 have an increase in mean currents of 46% after the anode change. At 15:25 the concentration of CF_4 drops with the change from underfeeding to overfeeding of alumina to the cell. This could possibly be an indication of a too low concentration of alumina during this period after the anode change.

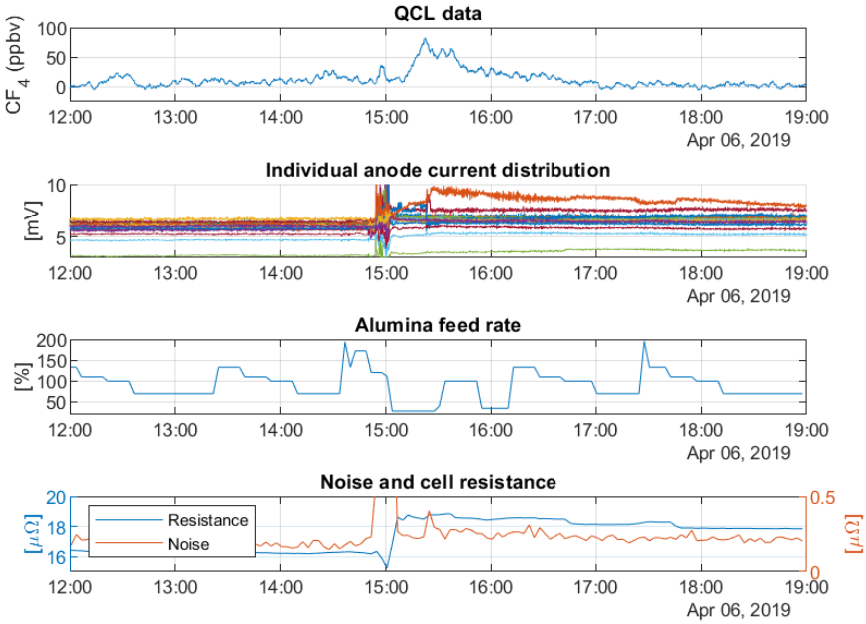

Figure 4.6: Case 3: at 15:00 the anodes in position 10-11 are being replaced.

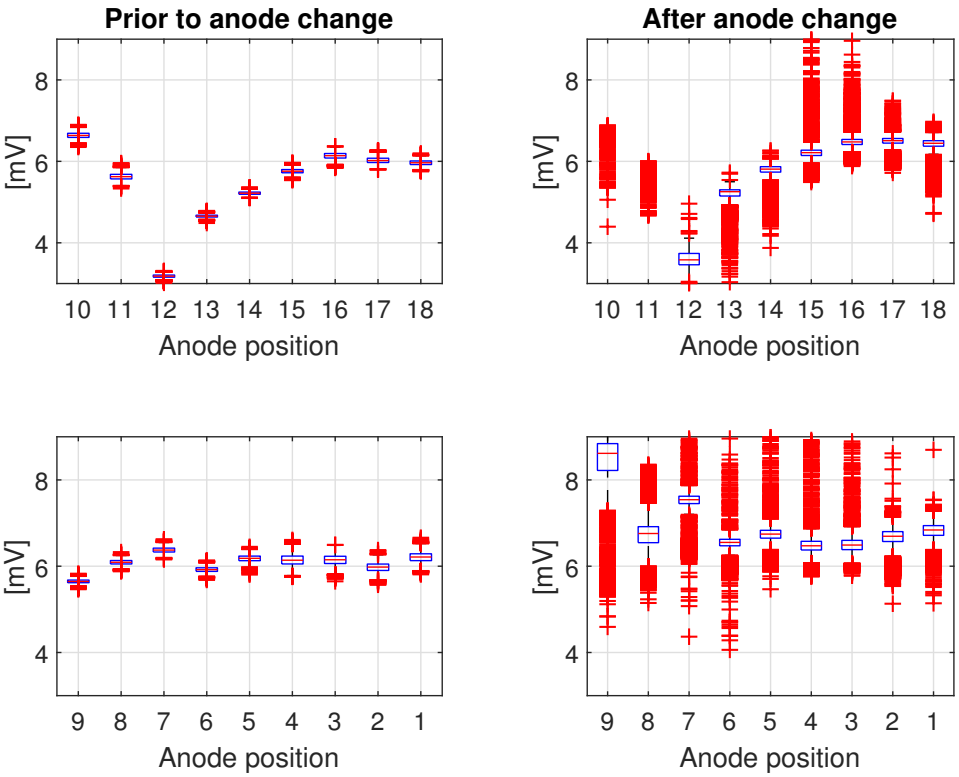

Figure 4.7: Case 3: Boxplots of individual anode currents over the period depicted in figure 4.6. Boxplots prior to anode change is from 12:00-15:00. Boxplots after anode change is from 15:00-19:00.

Case 4

In figure 4.8 leading up to 15:20, there is some spread in the anode current distribution measurements. This is also noticeable in figure 4.9 prior to the anode change. However, this does not affect the concentration of CF_4 as seen in figure 4.8. From 15:20-16:00 the cell gets an increase in the cell resistance. This is caused by an resistance modifier being added to the cell by an operator prior to the anode change. With the increase of cell resistance, the noise decrease a bit, leading up to the anode change. At 16:00 the anode change takes place and an increase in the concentration of CF_4 can be observed at the same time. In addition, there is a noticeable increase in the noise after the anode change. For this case the concentration of CF_4 is steady around 45 ppbv after the anode change.

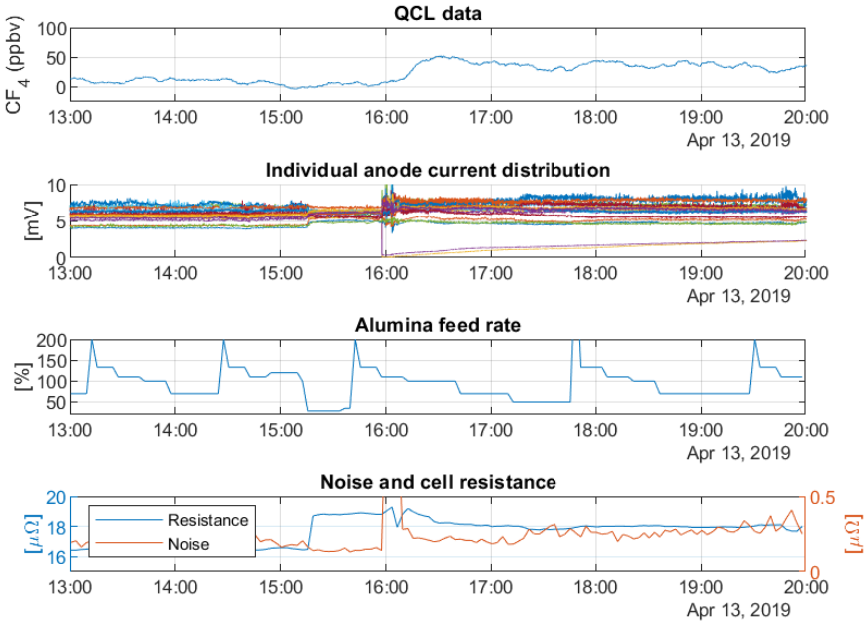

Figure 4.8: Case 4: at 16:00 the anodes in position 3-4 are being replaced.

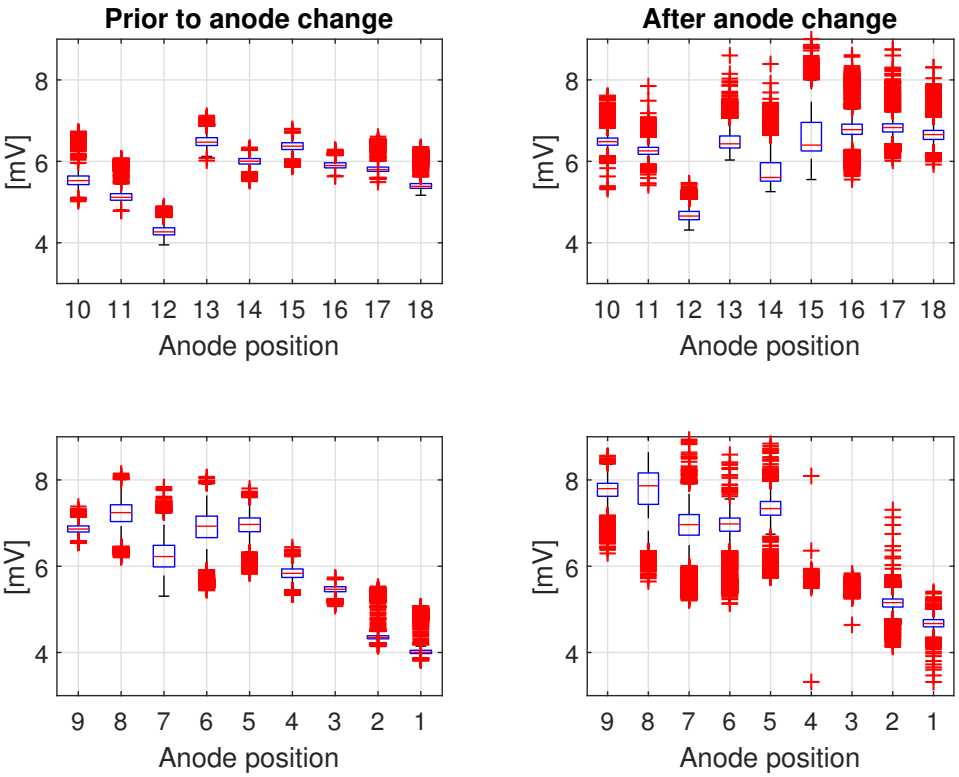

Figure 4.9: Case 4: Boxplots of individual anode currents over the period depicted in figure 4.8. Boxplots prior to anode change is from 13:00-16:00. Boxplots after anode change is from 16:00-20:00.

Case 5

In figure 4.10 leading up to the anode change at 16:30 the concentration of CF_4 decreases from a higher level. Why the concentration of CF_4 decreases prior to the anode change have not been studied in this case. Note that data for anode 12 is omitted due to a faulty sensor. The anodes in position 7-8 are being replaced in this case. During the anode change for this case, the QCL saturates. Why this happened is unknown, but from figure 4.11 extreme fluctuations in the currents can be observed for all of the anodes. From table 5 in the appendix, several anodes with peak currents in the range of 116 % - 142 % compared to the mean currents prior to the anode change can be observed. In addition, the anodes in position 10 and 11, opposite of the two being replaced, have an average increase in mean currents of 38 % and 47 % after the anode change, respectively. Since the cell noise is high after the anode change the cell does not enter an underfeeding period of alumina until 17:15. However, the concentration of CF_4 is steady around 70 ppbv after the anode change.

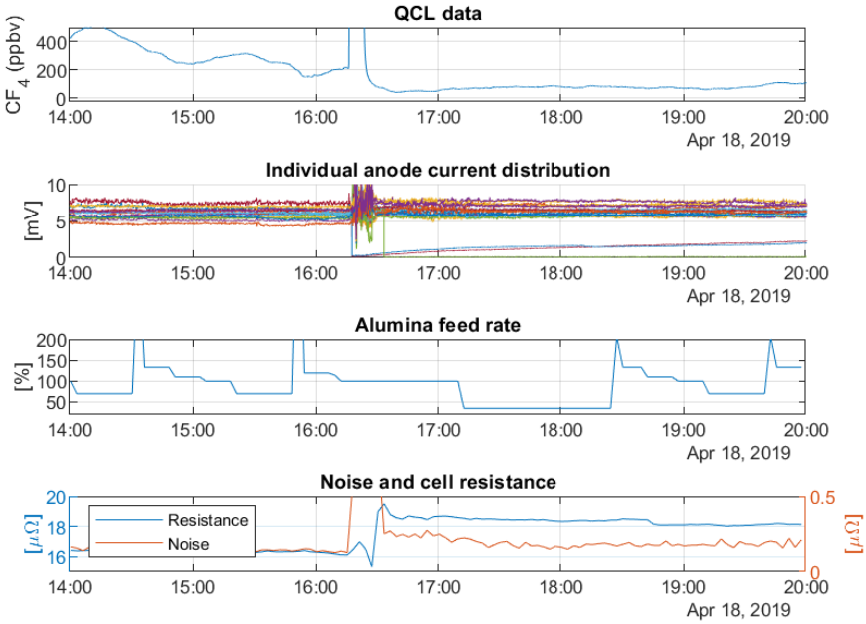

Figure 4.10: Case 5: at 16:00 the anodes in position 7-8 are being replaced.

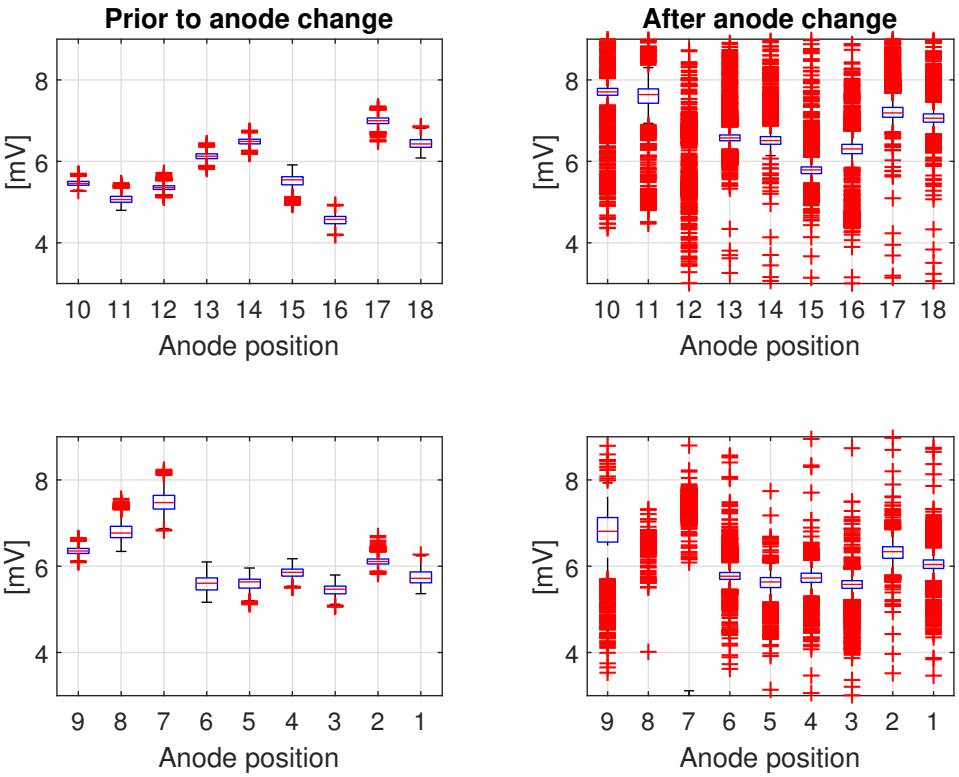

Figure 4.11: Case 5: Boxplots of individual anode currents over the period depicted in figure 4.10. Boxplots prior to anode change is from 14:00-16:30. Boxplots after anode change is from 16:30-20:00.

Case 6

In figure 4.12 it can be observed that the concentration of CF_4 decreases from a higher level because of previously operational problems in the cell. Leading up to the anode change at 15:45, the concentration of CF_4 decreases from a higher level because of previously operational problems. The anode in position 9 is the one being replaced in this case. This is an anode placed in the corner of the cell. From the time series in figure 4.12 it can be observed that none of the other anodes have any noticeable change in currents right after the anode change. There is a small increase of CF_4 during the anode change, however the concentration continues to decrease right after the anode change. Around 18:30 the currents through the anodes in position 8 and 16 starts to vary. this can also be observed in figure 4.13 as there are several outliers in the high range of currents through the anode. These variations is noticeable in the cell noise and in the concentration of CF_4 as they both increase.

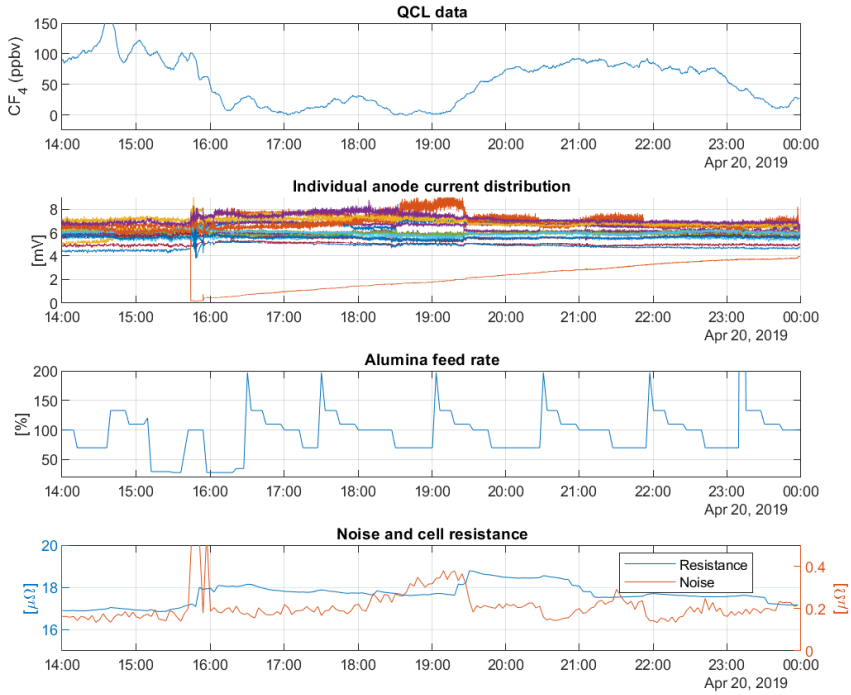

Figure 4.12: Case 6: at 15:45 the anode in position 9 is being replaced.

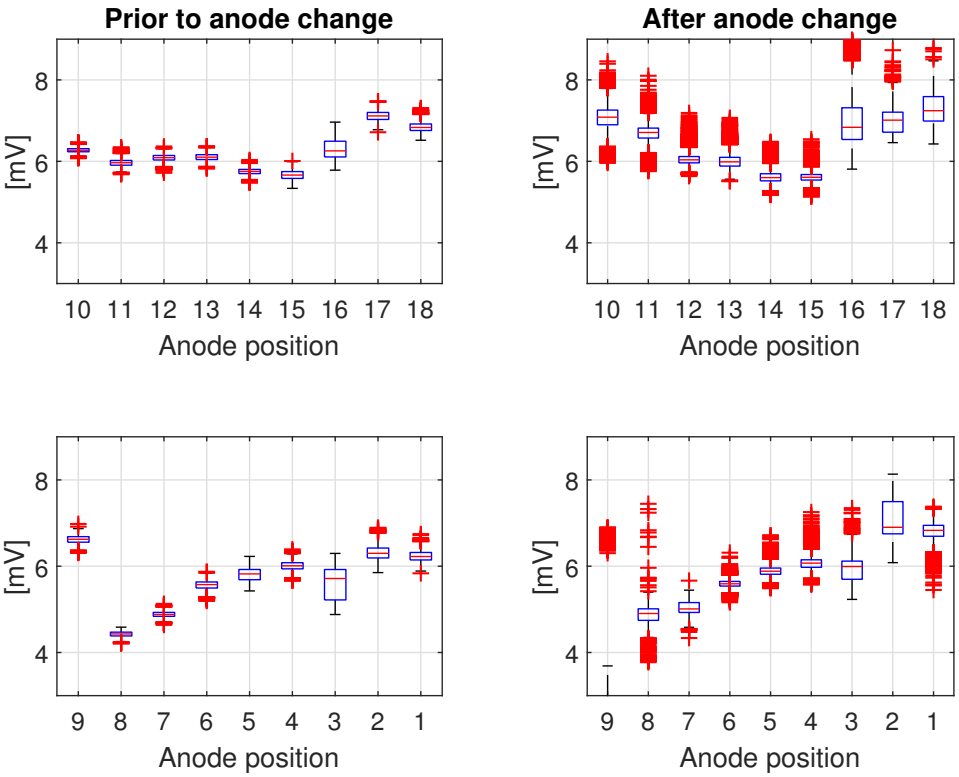

Figure 4.13: Case 6: Boxplots of individual anode currents over the period depicted in figure 4.12. Boxplots prior to anode change is from 14:00-15:45. Boxplots after anode change is from 15:45-00:00.

4.4.2 Anode problem/imbalance

Problem description

From time to time there can be operational problems with the anodes in the cell. There are many possible issues associated with anodes. Sludge at the cell bottom, spikes under the anode, locally wrong ACD and more. What these deviations have in common is that the ACD is affected locally, but also in some cases throughout the entire cell. If an operator notices any problems related to anodes, an action is being taken and logged in the process database. To collect data from these events, the process logs of the cell was monitored.

Results and discussion

Case 7

This case is an example of a cell being followed up by an operator after the anode change. From figure 4.14 it can be observed that the anode in position 18 is replaced at 15:40. From figure 4.16 it can be observed that anodes adjacent and opposite of the one being replaced

immediately starts to compensate for the lack of currents drawn by the new anode in the cell. From table 7 in the appendix an increase of around 20% in mean currents after the anode change for anode 1 and 16 can be observed. Because of this, the cell noise increases. In addition to the increase in cell noise, the concentration of CF_4 increases to around 65 ppbv at 17:00. At 18:30 an operator is trying to adjust the anodes in position 1, 16 and 17 to help remove the noise from the cell. This can be seen in figure 4.16. After adjusting the anodes (increasing the ACD), the currents through these anodes decrease with 14, 26 and 10 %, respectively. However, the anode in position 2 picks up an increase of 19 %, thus making the noise still present on the cell together with an steady concentration around 40 ppbv CF_4.

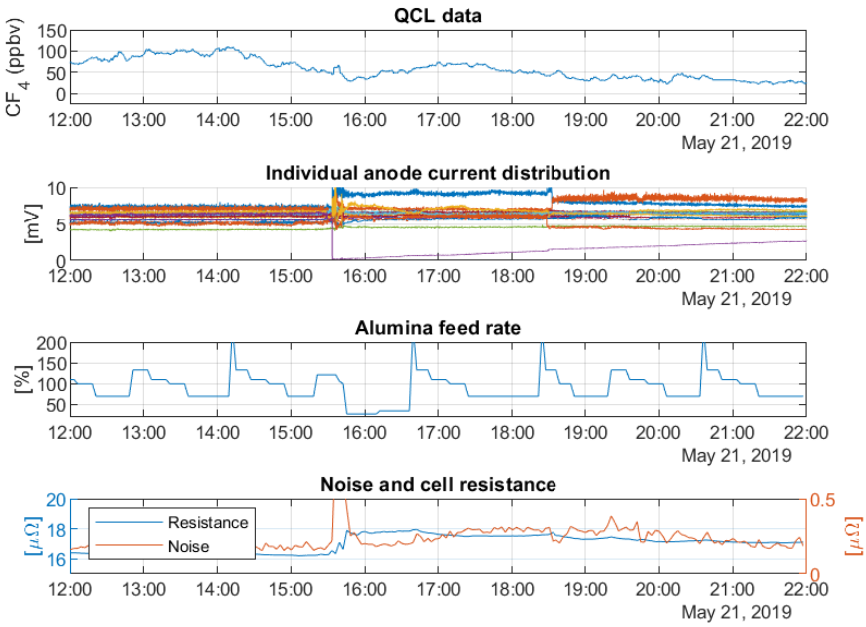

Figure 4.14: Case 7: at 15:40 the anode in position 18 is being replaced.

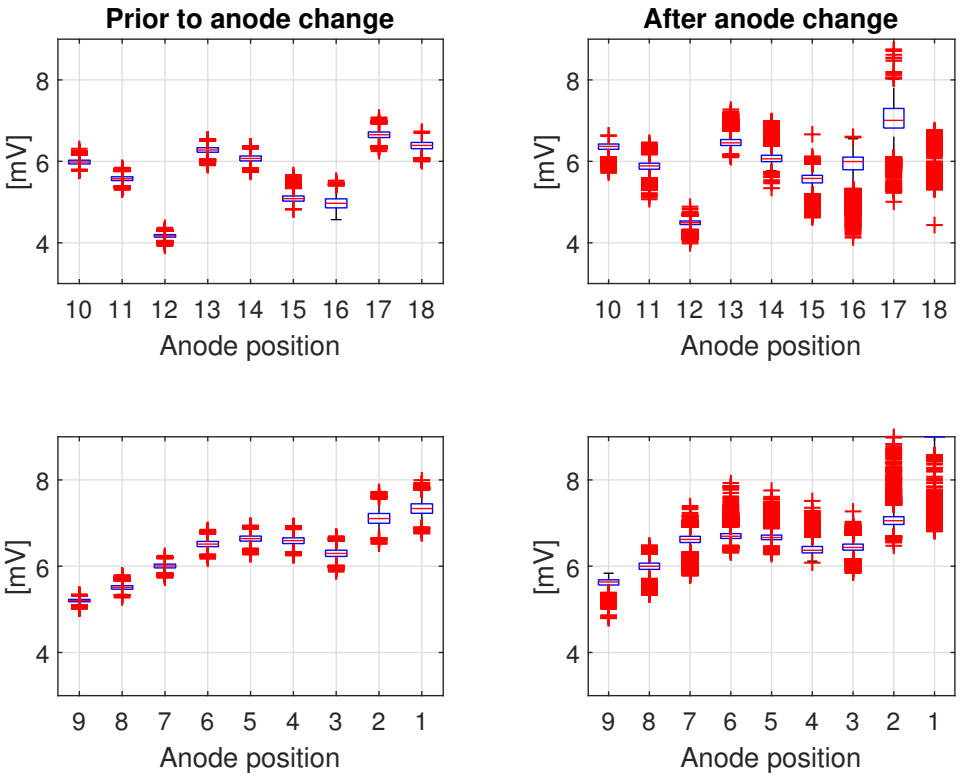

Figure 4.15: Case 7: Boxplots of individual anode currents over the period depicted in figure 4.14. Boxplots prior to anode change is from 12:00-15:20. Boxplots after anode change is from 15:20-18:20.

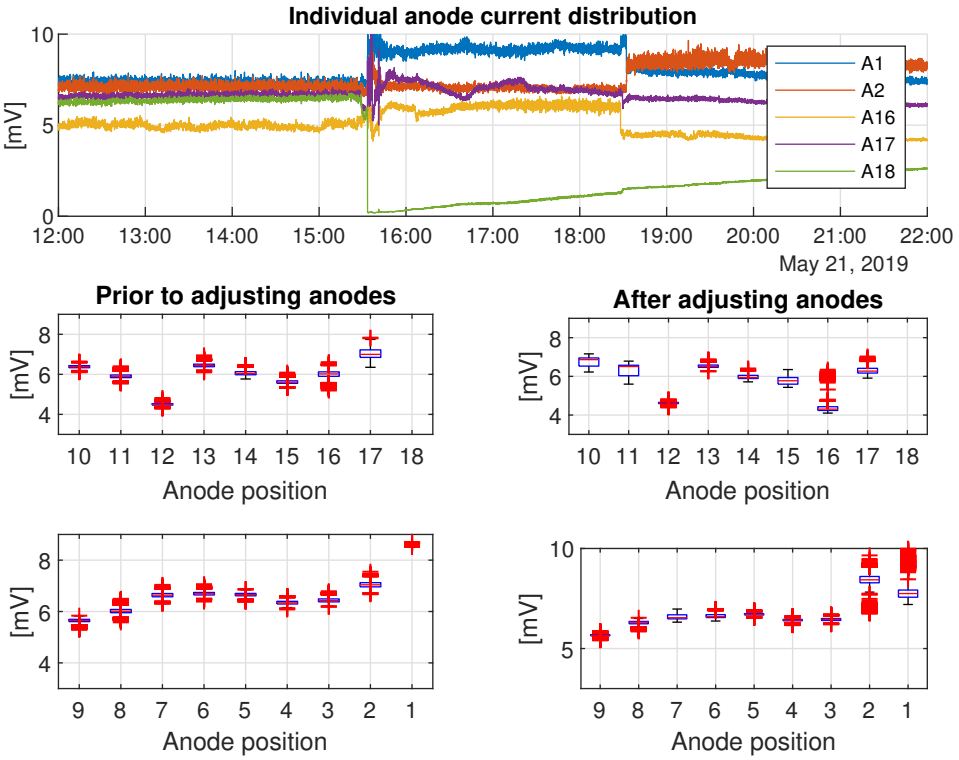

Figure 4.16: Case 7: extracted adjusted anodes. Boxplots prior to adjusting anodes is from 15:20-18:20. Boxplots after adjusting anodes is from 18:25-22:00

Case 8

Note that in figure 4.17 QCL data is missing from 05:00 to 10:30. This case is almost equal to case 7. From figure 4.17 it can be observed that at 10:45 the anode in position 2 is being adjusted (increasing the ACD) probably due to fluctuations in the currents through this anode. However, immediately after the adjustment the currents through the anodes in position 13 and 14 starts to vary, see figure 4.18 and figure 4.19. At 11:30 the anodes in position 13 and 14 are being adjusted accordingly. However, the anode in position 15 is let out, even if its shows signs of fluctuation in the currents. The variation in currents through anode 15 keeps the cell noise increased, together with an steady concentration CF_4 around 50 ppbv .

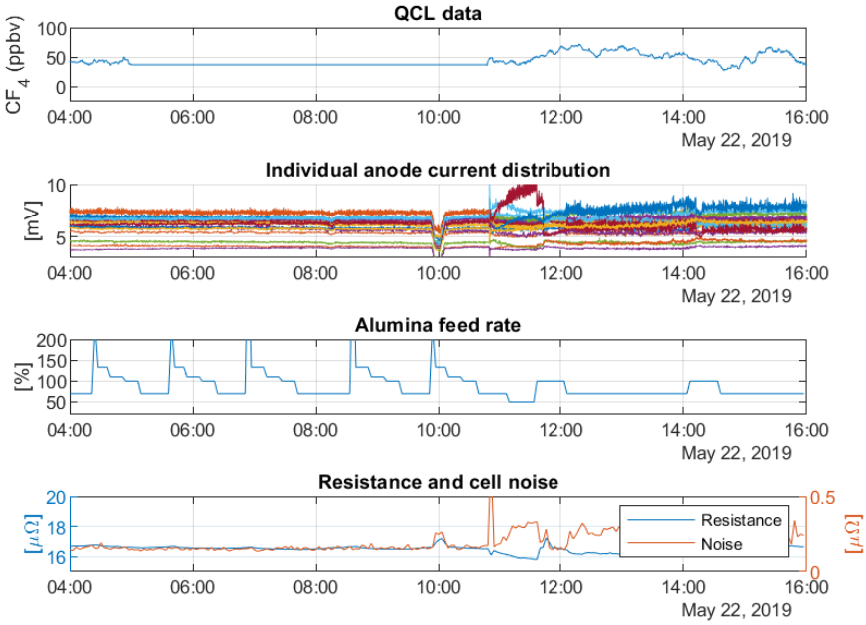

Figure 4.17: Case 8: insufficient adjustment of anodes in position 13-14.

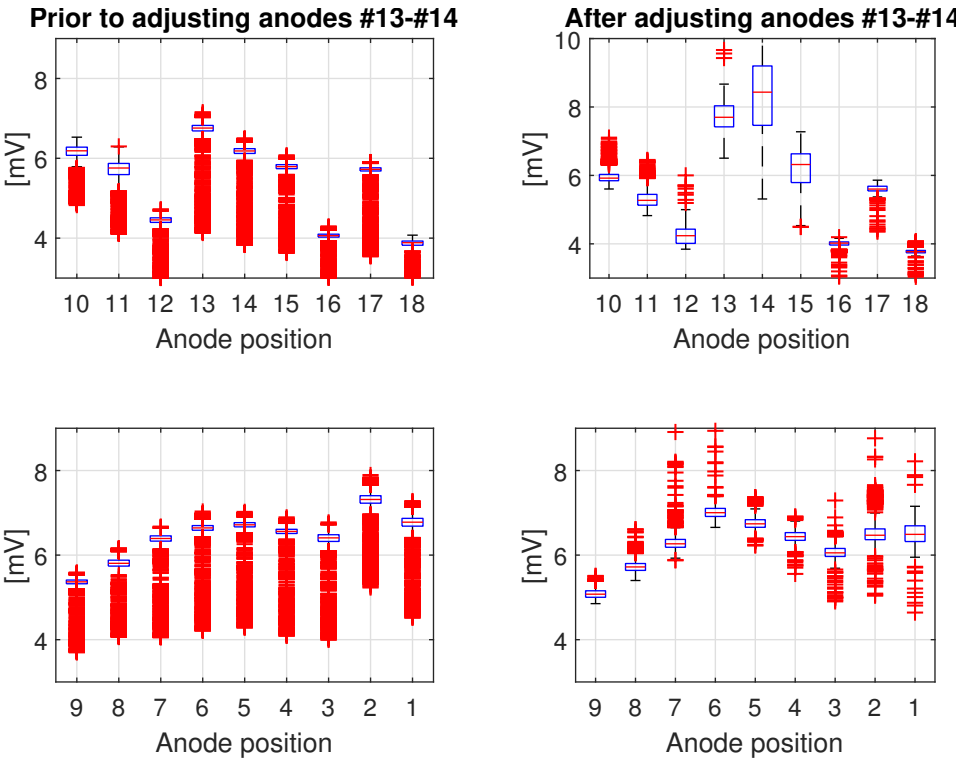

Figure 4.18: Case 8: Boxplots of individual anode currents over the period depicted in figure 4.17. Boxplots prior to anode adjustment is from 04:00-10:45. Boxplots after adjustment is from 10:45-11:30.

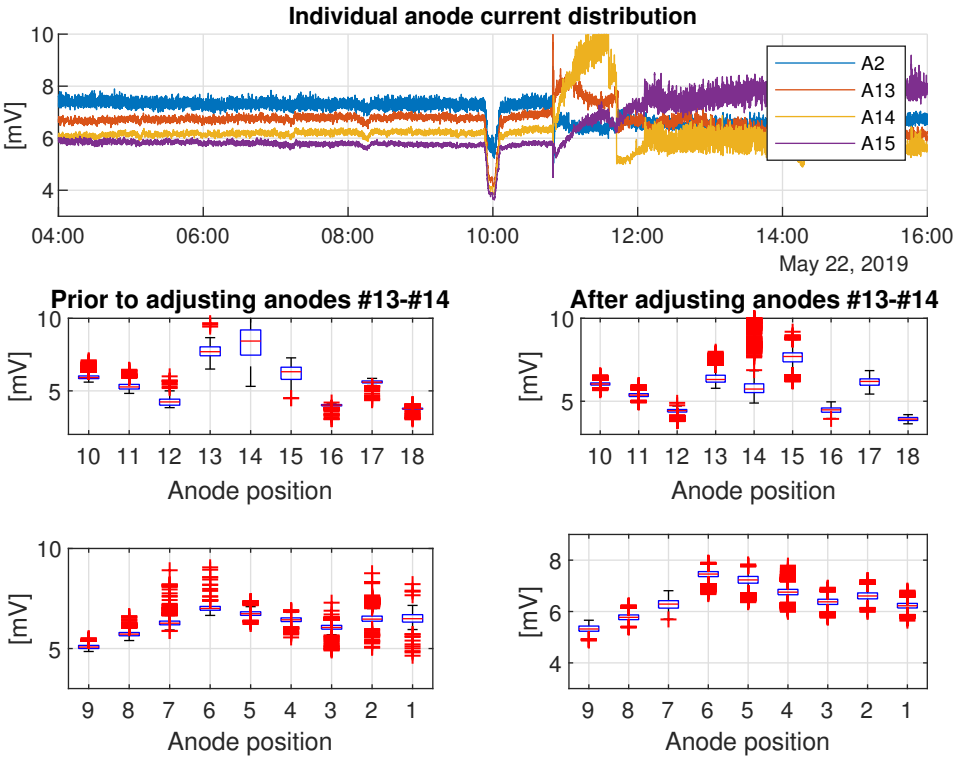

Figure 4.19: Case 8: extracted adjusted anodes. Boxplots prior to adjusting anodes is from 10:45-11:30. Boxplots after adjusting anodes is from 11:30-16:00

Case 9

In figure 4.20 the deviating individual anode currents have all ready been extracted. From both the time series and the boxplots in figure 4.21 it is easy to spot the two deviating anodes prior to any adjustments. Accordingly, the cell noise and concentration of CF_4 is high. At 01:00 the anodes in position 3 and 4 are being adjusted (increasing the ACD). During the adjustment of the anodes the QCL saturates. As the action of increasing the ACD of anode 3 and 4 becomes visible, a decrease in both CF_4 and cell noise can be observed around 02:30. From 03:00-05:30 there is some fluctuation in currents through the anodes in position 5 and 6. In this period there also is noticeable cell noise and an increased production of CF_4. When the fluctuations in currents through anode 5 and 6 settles at 05:30, the cell noise and concentration of CF_4 decrease accordingly.

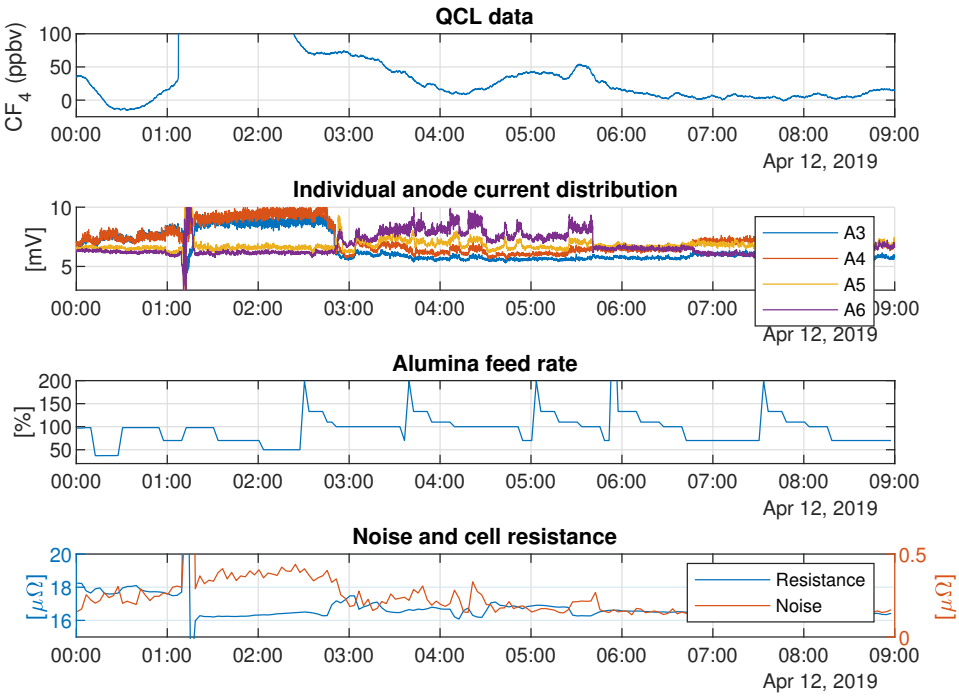

Figure 4.20: Case 9: correct adjustment of anodes in position 3-4.

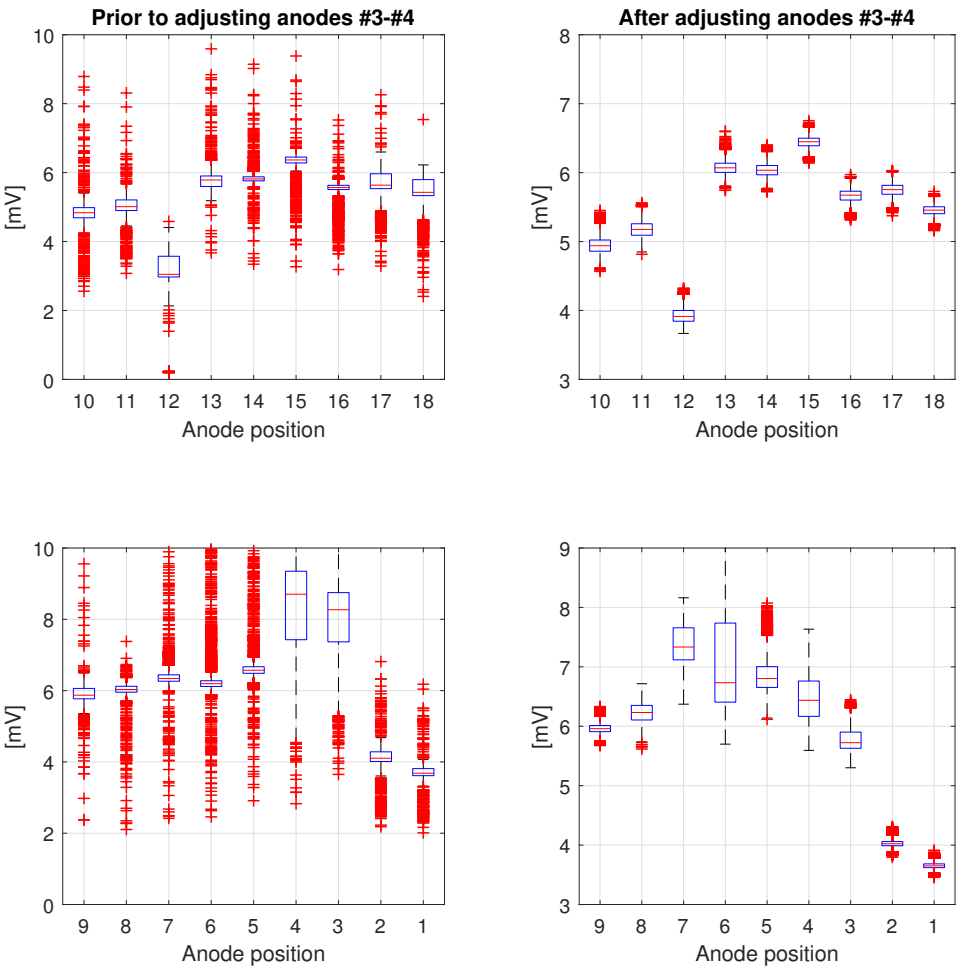

Figure 4.21: Case 9: Boxplots of individual anode currents over the period depicted in figure 4.17. Boxplots prior to anode adjustment is from 00:00-03:00. Boxplots after adjustment is from 03:00-09:00.

4.4.3 Preheated anodes

Problem description

At the same time as this project was carried through, another student also carried out his own measurements related to preheating of anodes. The anodes were preheated by placing them between old and hot anodes taken from other cells. They were heated to a core temperature around 150°C before they were placed in the test cell. There are several interesting results to look for with preheating of anodes, specially how the preheating affects the anode current distribution and co-evolution of PFCs. If the anodes start to pick up current faster, this can possibly lower the cell noise caused by an non-uniform anode

current distribution.

Results and discussion

Case 10

Unfortunately the cell noise was not extracted during this period, but the value of the cell noise modifier. This is a modifier that is being added to the cell resistance if the calculated cell noise is over a set limit. However, from figure 4.22 it can be observed that the cell is stable leading up to the anode change at 16:00. From both the anode current time series and the boxplots in figure 4.23 an uniform current distribution can be observed. The concentration of CF_4 is also under the LOD leading up to the anode change at 16:00. The anodes in position 7 and 8 are replaced. After the anode change, from 16:00-16:50 there is an increase in the concentration of CF_4. At 16:50 the concentration of CF_4 drops with the change from underfeeding to overfeeding of alumina to the cell. This could be an indication of low concentrations of alumina during this period after the anode change. There are no obvious signs of improvement of preheating the anodes in this case, regarding the anode current distribution.

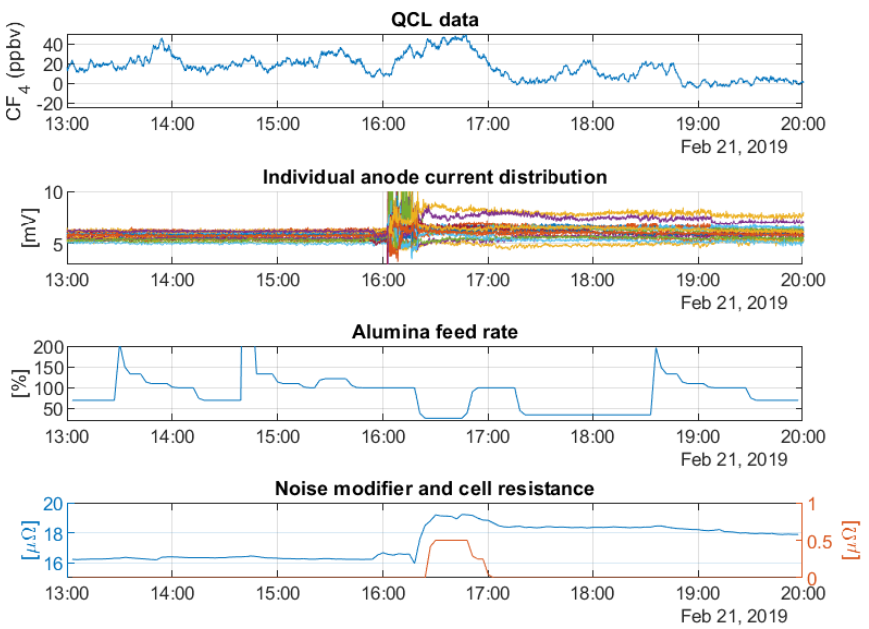

Figure 4.22: Case 10: cell response to changing anodes in position 7-8 (preheated anodes to 150°C).

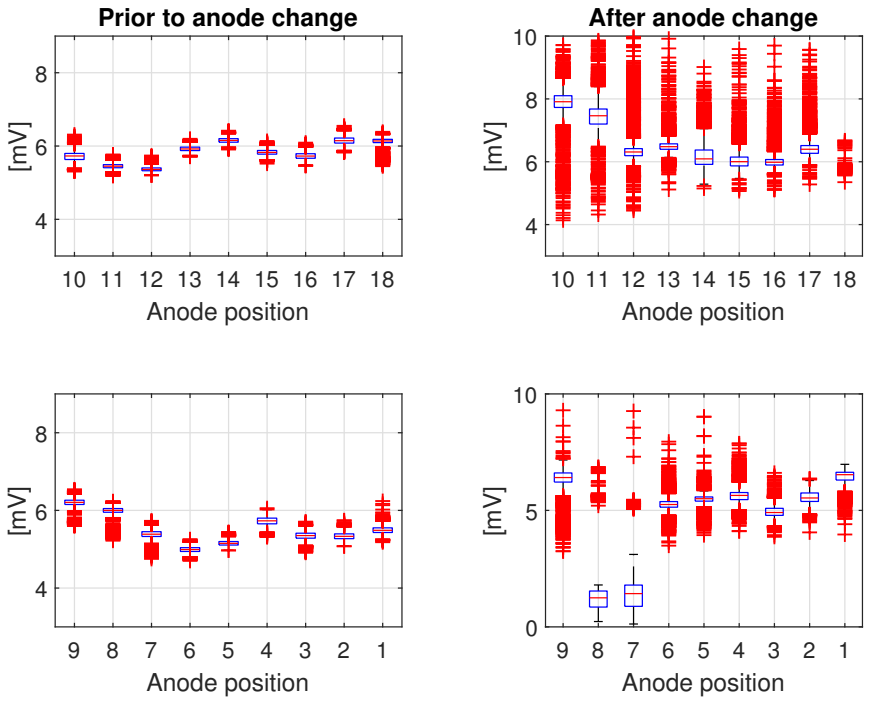

Figure 4.23: Case 10: boxplots of individual anode currents over the period depicted in figure 4.22. Boxplots prior to anode change is from 13:00-16:00. Boxplots after anode change is from 16:00-12:00.

Case 11

Note that data for anode 12 is omitted due to a faulty sensor. As can be seen in figure 4.24 leading up to the anode change at 15:45 the cell has no operational problems and is stable. With the start of the anode change there is a peak increase in the concentration of CF_4. From table 11 in the appendix it can be observed that the anodes in position 5 and 6 have peak currents of 101% and 122% compared to average currents prior to the anode change. These peak currents can also be seen in figure 4.25 as outliers in the higher end. In addition, anode 5 and 6 have an average increase in current of 18% and 20% after the anode change. The concentration of CF_4 in this period is steady around 65 ppbv. There are no obvious signs of improvement of preheating the anodes in this case either.

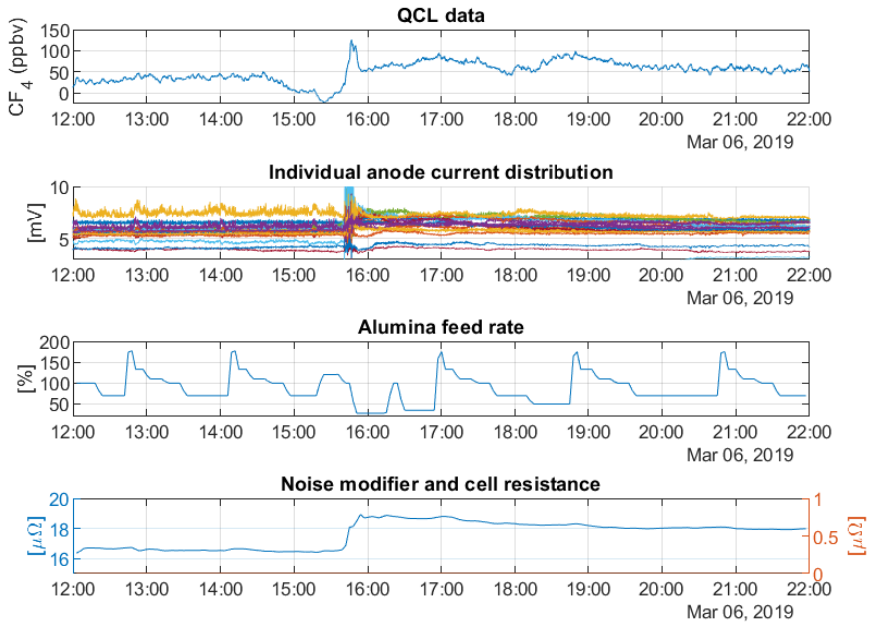

Figure 4.24: Case 11: cell response to changing anodes in position 12-13 (preheated anodes to 150°C).

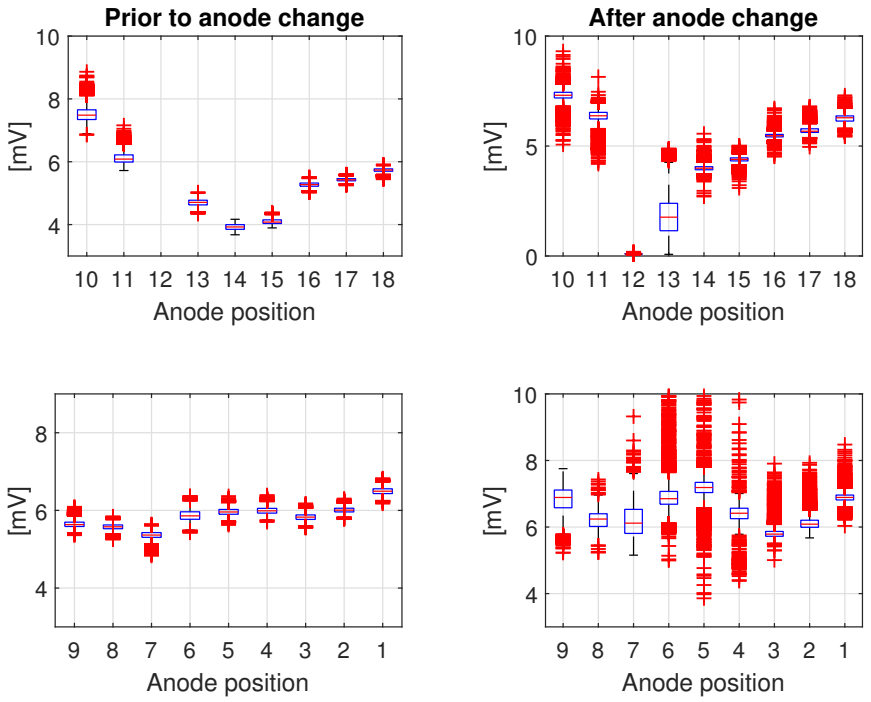

Figure 4.25: Case 11: boxplots of individual anode currents over the period depicted in figure 4.24. Boxplots prior to anode change is from 12:00-15:45. Boxplots after anode change is from 15:45-22:00.

4.5 Analysis of PFC emissions during different alumina feed settings

4.5.1 Problem description

The alumina concentration is obtained by altering between an overfeed- and underfeeding period. This is done so the alumina feed control algorithm can look for a change in pseudo-resistance, or a change in the slope of the pseudo-resistance versus alumina concentration curve, while the alumina concentration in the cell is moved in a specific direction. For the smelter location of this thesis, the resistance slope is used to determine when to stop an underfeeding period, and to initiate overfeeding. As mentioned, the resistance slope terminates the underfeeding when it reaches a specified limit. This is done to prevent the concentration of alumina to become too low in the electrolyte. If the concentration of alumina in the electrolyte becomes too low, the risk of an conventional AE is present as mentioned earlier. However, concentration gradients of alumina can still be present in the electrolyte without an AE present. If the resistance slope target is set too high, this allows the cell to become starved of alumina. This can possibly cause an increase in the production of PFC from the electrolysis cell. In the following sections various experiments

have been performed to see how various feed settings affects production of PFC in an electrolysis cell.

4.5.2 Results and discussion

Normal alumina feed cycling

In figure 4.26 it can be seen how the resistance slope terminates the underfeeding periods when it reaches its set limit. By looking at the resistance slope together with the concentration of CF_4 it is evident that the concentration of CF_4 increases with rising resistance slope. This is an indication of low alumina concentration during the end of the underfeeding periods. During the period from 00:00 to 06:30 there also is some cell noise present, and during this period the concentration of CF_4 do reach higher values compared to the period from 06:30 to 13:00. In figure 4.27 the anode in position 4 stands out compared to the rest, and in figure 4.28 the boxplots for the given time period is shown. For the anode in position 4 the median value of currents through the anode increases a small amount in the period from 06:30 to 13:00. However, there are not as many extreme outliers compared to the period before, thus less cell noise and lower values of CF_4.

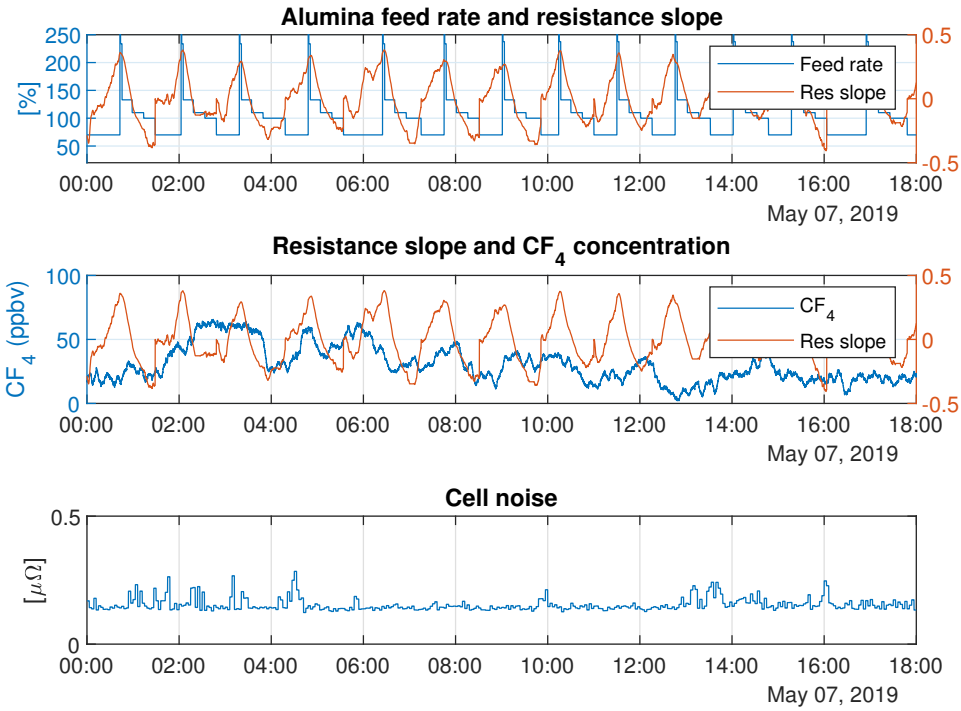

Figure 4.26: Top plot: alumina feed rate together with the resistance slope. Middle plot: concentration of CF_4 compared to the resistance slope. Bottom plot: cell noise.

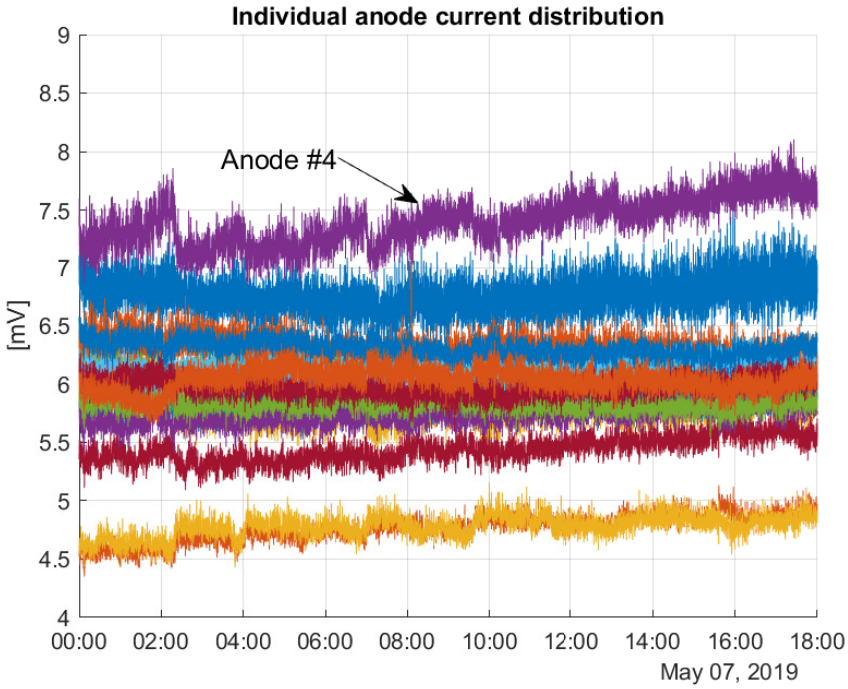

Figure 4.27: Higher currents through anode #4.

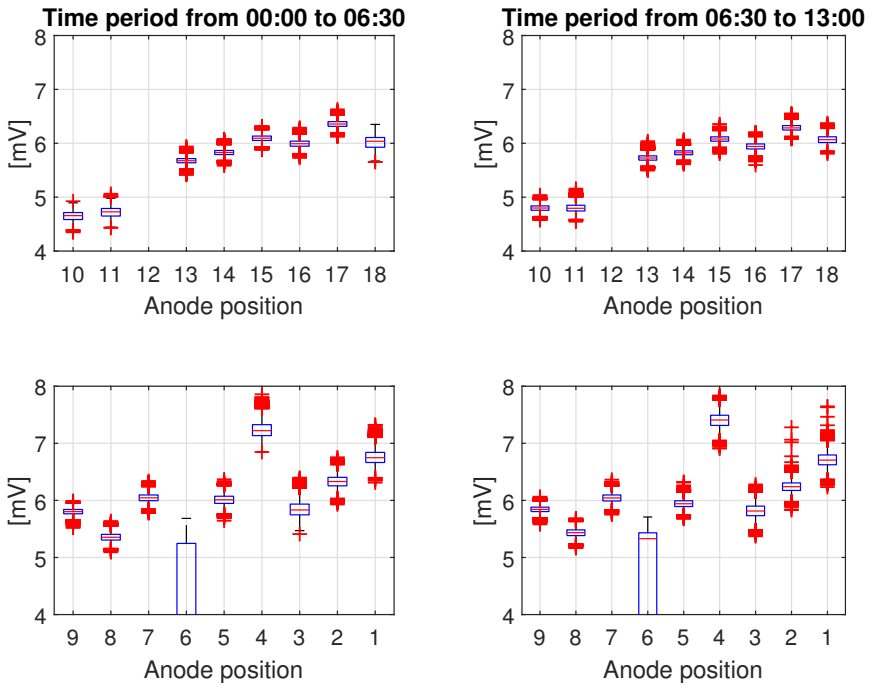

Figure 4.28: boxplots of individual anode currents over the period 00:00 - 13:00. Boxplots to the left is from 00:00 to 06:30. Boxplots to the right is from 06:30 to 13:00. Note that data for the anode in position 6 is omitted due to a faulty sensor

In figure 4.29 an example of a noisy cell is shown. For the time period from 06:00 to 10:00 and from 12:00 to 14:30 the cell noise is high. During these periods there is a lot of noise in the resistance slope as well, making it difficult for the alumina feeding algorithm to calculate the correct resistance slope. Leading up to the first period of noise the concentration of CF_4 is high, but from 05:00 the concentration of CF_4 decreases from around 350 ppbv to 100 ppbv. This indicates that the cell has gained access to a higher amount of alumina at this point. This can possibly be from lumps of alumina falling into the electrolyte without the entire amount dissolving. The undissolved alumina will settle at the bottom of the cell, causing a non-uniform current distribution through some of the anodes. Here it would be ideal to show the anode current distribution, but unfortunately the instrument malfunctioned during this period of time. However, in the period from 10:00 to 12:00 the process control system notices the noise and adds a temporary resistance modifier to increase the cell resistance target. This causes the noise to decrease during this period. When the resistance modifier is removed, the noise returns and the concentration of CF_4 increases again. This supports the explanation of undissolved alumina temporary settling at the bottom, causing a non-uniform anode current distribution. From 15:30 there is an anode change. After the anode change, a temporary resistance modifier is added to the cell resistance, thus removing the noise and the increased levels of CF_4.

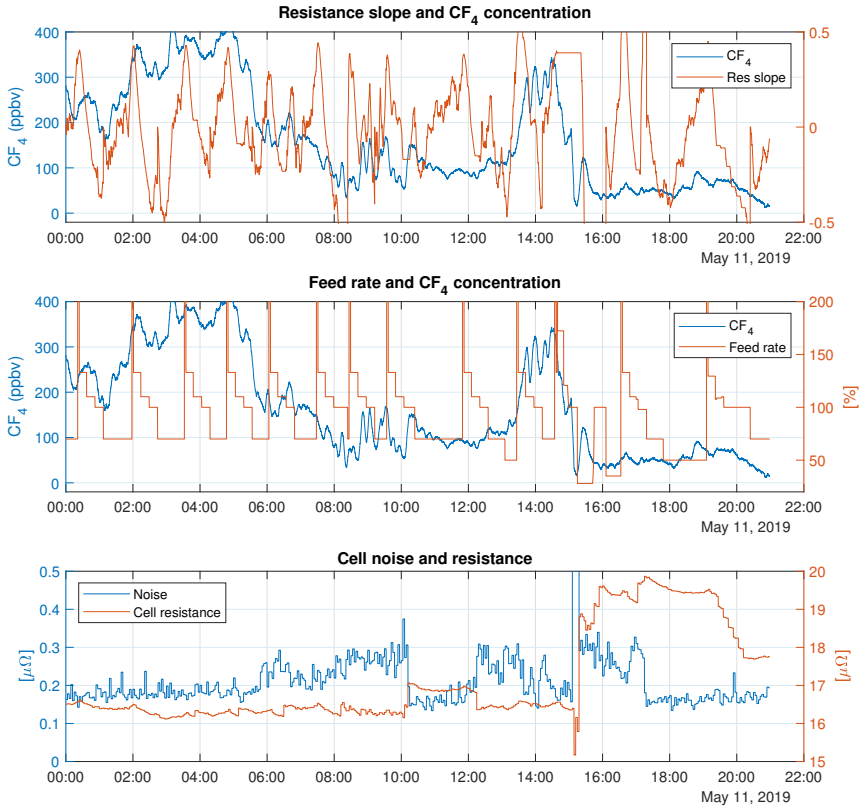

Figure 4.29: Concentration of CF_4 compared to resistance slope and feed rate. Bottom plot shows cell noise and resistance during the same period of time.

Aggressive underfeed of alumina

Aggressive underfeed is an option the operators can use if they have suspicions of too much alumina in the cell. By activating aggressive underfeed from the cell control, the termination target of the resistance slope is increased. In figure 4.30 the cell was set in an aggressive underfeed in the period from 16:20 to 16:50 and 20:00 to 20:25. Leading up to the first aggressive underfeed the concentration of CF_4 all ready follows the resistance slope, and there are no signs of elevated emissions during the first aggressive underfeed. For the next aggressive underfeeding period the concentration of CF_4 rises abruptly during the end of the underfeed. In fact, for this last underfeed the pot probably would had an AE if the underfeeding period was not terminated at this point. Overall, this is an indication of the cell being operated in the lower range of alumina concentration in the electrolyte. This could possibly explain the continuous concentration of CF_4 during this entire period.

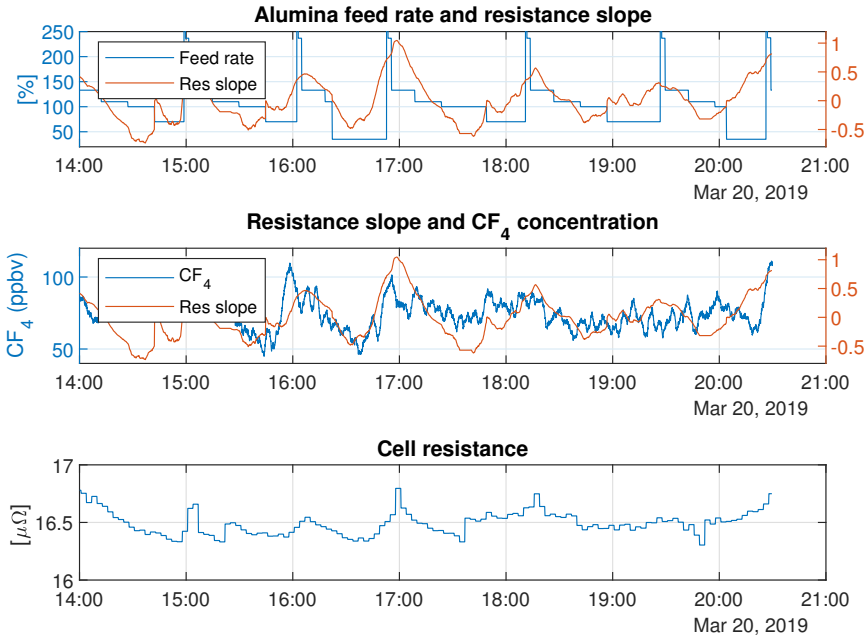

Figure 4.30: Top plot: alumina feed rate together with the resistance slope. Middle plot: concentration of CF_4 compared to the resistance slope. Bottom plot: cell resistance.

Increased resistance slope target

In figure 4.31 the resistance slope target is increased by 20 %. This is much like an aggressive underfeed, except from the slope target is lower than it is for an aggressive underfeed. During this period there are no obvious disadvantages of an increased slope target. The concentration of CF_4 still correlates with the resistance slope, with higher consecrations during the end of the underfeeding periods.

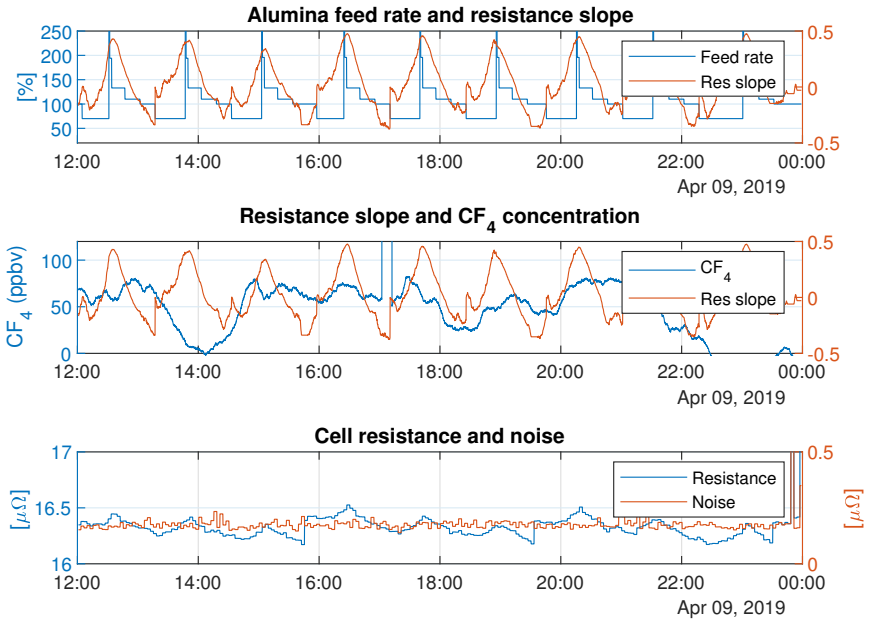

Figure 4.31: Top plot: alumina feed rate together with the resistance slope. Middle plot: concentration of CF_4 compared to the resistance slope. Bottom plot: cell resistance and noise.

Chapter 5

Overall summary, conclusion and future work

In the present thesis co-evolution of PFC gases from a prebake electrolysis cell has been investigated. The goal of this study have been to contribute to the knowledge of when these emissions are present, and how they can be mitigated in the industrial electrolysis process. In hindsight of the experiments and results presented in this thesis, there are several interesting findings. To summarize and evaluate the results, the goal of the thesis as stated in section 1 is used.

5.1 Summary and conclusion

From monitoring the process over a long time, it is apparent that a non-uniform anode current distribution leads to higher concentrations of PFCs. A non-uniform anode current distribution is often present during anode change and right after the anode change is completed. Anodes adjacent and opposite of the one anode(s) being replaced often compensate for the lack of currents drawn by the new and cold anode(s) in the cell. In this study there were several anodes with an average increase in currents ranging from 15 % to 46 % after the anode change was completed. In addition, there were several peak currents over 100 % in the same period. With currents this high, the risk of exceeding the CCD is present.

In addition to increased levels of CF_4 during a non-uniform current distribution, the feeding of alumina to the electrolyte also affects the production of CF_4. When the concentration of alumina is at an adequate level, it has been observed that the formation of CF_4 follows the resistance slope down to the LOD of the QCL. In cases of small concentrations of alumina in the electrolyte, typically in the end of an underfeeding period when resistance curve slopes are high, the production of CF_4 is sensitive to noise, as seen in figure 4.26.

The process control at this smelter already have a well developed system to handle both undesirable and planned events. However, the process control have not been designed with

these small concentrations of PFCs in mind. The reason of this is mainly caused by the of lack of instruments to do these types of measurements. By use of the QCL used in this thesis in addition to the individual anode current measurements, the process control can be tuned to handle the events of elevated production of PFC. This can be done by altering the different limits and set points in the process, while monitoring the response.

Except from the process control system, the operators working in the smelters have a big impact on the process. If they utilize their expertise, they can contribute to lower the overall PFC emissions. The process control can not operate to its full extent, unless the manual tasks are done properly. In addition, when the process control is insufficient to fix a problem, the operators have to find and execute the correct measures.

5.2 Future work

The next step of this work is to utilize the knowledge of when the PFC emissions occurs. New experiments should be designed based on tuning the process control, especially the feed control. One must ensure that the concentration of alumina in the electrolyte and under all the anodes is sufficient at all time. In addition, find or develop a method to ensure that the anodes do not exceed their CCD during a non-uniform current distribution in the electrolysis cell.

Bibliography

Aarhaug, T. A., 2019. Online monitoring of perfluorcarbon (PFC) emissions from aluminium industry. https://blog.sintef.com/industry-en/online-monitoring-pfc-emissions-aluminium-industry/, (Accessed: 20.05.19).

Aarhaug, T. A., Ferber, A., Gaertner, H., Kolås, S., Ryman, S. O., Geiser, P., 2018. Validation of Online Monitoring of PFC by QCL with FTIR Spectroscopy. TMS Light Metals, pages 1487–1493.

Batista, E., Dando, R. N., Menegazzo, N., Espinoza-Nava, L., 2016. Sustainable reduction of anode effect and low voltage PFC emissions. TMS Light Metals, pages 537–540.

Espinoza-Nava, L., Menegazzo, N., Dando, N. R., Geiser, P., 2016. QCL-based perfluorocarbon emission monitoring. TMS Light Metals, pages 541–544.

Grjotheim, K., Kvande, H., 1993. Introduction to aluminium electrolysis, 2nd Edition. Aluminium-Verlag.

Hanssen, A., 2018. Formation of PFC in an electrolysis cell by use of a Quantum Cascade Laser. Tech. rep., Departement of Engineering Cybernetics, NTNU.

Hestetun, K., 2009. Use of data from anode current distribution for state and parameter estimation and fault detection in an aluminium prebake electrolysis cell. Ph.D. thesis, NTNU.

IAI, 2018. The international aluminium institute. http://primary.world-aluminium.org/index.php?id=286&L=0, (Accessed: 11.11.18).

Kvande, H., Drabløs, P. A., May 2014. The Aluminum Smelting Process and Innovative Alternative Technologies. Journal of occupational and environmental medicine 56 (5), S23.

Marks, J., Bayliss, C., 2012. GHG Measurement and Inventory for Aluminum Production. TMS Light Metals, pages 805–808.

NeoMonitors, 2018. LaserGas™ Q - QCL Edition - User's reference 1.0. Neo Monitors, http://neomonitors.com/tdls-dust-and-gas-analyzers/lasergas-q-cf4/.

Pedersen, B., 2018. Store norske leksikon - Aluminium. `https://snl.no/aluminium`, (Accessed: 10.03.19).

Rye, Å. K., Königsson, M., Solberg, I., 1998. Current redistribution among individual anode carbons in a Hall-Heroult prebake cell at low alumina concentrations. TMS Light Metals.

Tarcy, G., Tabereaux, A., 2011. The Initiation, Propagation and Termination of Anode Effects in Hall-Héroult Cells. TMS Light Metals, pages 329–332.

Thonstad, J., Utigard, T., Vogt, H., 2000. On the anode effect in aluminium electrolysis. TMS Light Metals, pages 131–138.

Whitfield, D., Skyllas-Kazacos, M., Welch, B., McFadden, S. F., 2004. Aspects of alumina control in aluminium reduction cells. TMS Light Metals, pages 249–255.

Wong, D. S., Tabereaux, A., Lavoie, P., 2014. Anode effect phenomena during conventional AEs, low voltage propagating AEs & non-propagating AEs. TMS Light Metals, pages 529–534.

Åsheim, H., 2017. PFC Evolution in the Aluminium Production Process. Ph.D. thesis, NTNU.

Appendices

A Change in individual anode currents prior to and after anode change

Table 1: Case 1: change in anode currents prior to and after anode change.

Anode #	Change in mean currents prior to and after anode change [%]	Difference between mean currents prior to and peak currents after anode change [%]
1	7	33
2	6	18
3	9	26
4	11	57
5	10	68
6	29	63
7	13	49
8	7	24
9	10	17
10	8	20
11	3	9
12	3	17
13	14	45
14	-76	5
15	-75	5
16	14	39
17	11	19
18	9	16

Table 2: Case 2: change in anode currents prior to and after anode change.

Anode #	Change in mean currents prior to and after anode change [%]	Difference between mean currents prior to and peak currents after anode change [%]
1	8	38
2	7	32
3	3	53
4	9	88
5	16	98
6	-16	47
7	23	90
8	18	36
9	16	24
10	9	18
11	11	22
12	-79	13
13	-76	5
14	2	56
15	4	24
16	4	20
17	4	19
18	8	23

Table 3: Case 3: change in anode currents prior to and after anode change.

Anode #	Change in mean currents prior to and after anode change [%]	Difference between mean currents prior to and peak currents after anode change [%]
1	9	51
2	11	44
3	6	109
4	6	111
5	9	100
6	10	51
7	17	75
8	11	37
9	46	91
10	-84	4
11	-73	7
12	12	56
13	11	23
14	10	20
15	8	98
16	6	66
17	7	24
18	7	17

Table 4: Case 4: change in anode currents prior to and after anode change.

Anode #	Change in mean currents prior to and after anode change [%]	Difference between mean currents prior to and peak currents after anode change [%]
1	15	32
2	16	65
3	-68	7
4	5	39
5	0	74
6	10	48
7	7	47
8	12	36
9	16	25
10	21	36
11	9	51
12	0	27
13	0	33
14	-4	40
15	3	58
16	14	46
17	16	50
18	22	52

Table 5: Case 5: change in anode currents prior to and after anode change.

Anode #	Change in mean currents prior to and after anode change [%]	Difference between mean currents prior to and peak currents after anode change [%]
1	5	129
2	3	78
3	2	80
4	-2	65
5	0	116
6	3	93
7	-76	18
8	-74	8
9	7	38
10	38	142
11	47	160
12	-84	115
13	7	59
14	1	60
15	5	85
16	37	124
17	4	75
18	10	89

Table 6: Case 6: change in anode currents prior to and after anode change.

Anode #	Change in mean currents prior to and after anode change [%]	Difference between mean currents prior to and peak currents after anode change [%]
1	9	18
2	12	29
3	6	31
4	1	21
5	1	16
6	1	14
7	3	16
8	10	68
9	-67	4
10	13	35
11	12	36
12	-1	18
13	-2	16
14	-2	13
15	-1	15
16	11	51
17	-2	32
18	7	28

B Change in individual anode currents prior to and after adjusting anodes

Table 7: Case 7: incorrect adjustment of anodes in position 1 and 16-17

Anode #	Change in mean currents prior to and after anode change [%]	Difference between mean currents prior to and peak currents after anode change [%]	Difference between mean currents after anode change and after adjusting anodes [%]
1	23	12	-14
2	0	9	19
3	2	7	0
4	-3	8	0
5	1	8	0
6	3	8	-1
7	10	7	0
8	8	6	5
9	7	6	1
10	6	7	7
11	5	6	8
12	7	5	3
13	3	7	1
14	0	7	-2
15	9	7	5
16	19	7	-26
17	6	12	-10
18	-83	7	83

Table 8: Case 8: incorrect adjustment of anodes in position 13-14.

Anode #	Change in mean currents prior to and after adjusting anode #2 [%]	Difference between mean currents prior to and peak currents after adjusting anode #2 [%]	Difference between mean currents after adjusting anode #2 and after adjusting anodes #14-#15 [%]
1	-4	22	-4
2	-10	20	1
3	-5	15	5
4	-1	6	5
5	1	10	7
6	6	37	6
7	-1	40	-1
8	-1	14	1
9	-4	3	5
10	-3	15	1
11	-7	13	1
12	-4	36	4
13	15	64	-17
14	35	69	-29
15	8	27	23
16	-1	4	12
17	-1	3	10
18	-2	6	4

Table 9: Case 9: correct adjustment of anodes in position 3-4

Anode #	Change in mean currents prior to and after adjusting anode #3-#4 [%]	Difference between mean currents prior to and peak currents after adjusting anode #3-#4 [%]
1	-1	6
2	0	4
3	-28	-19
4	-22	-9
5	3	21
6	12	59
7	15	28
8	3	12
9	1	7
10	2	13
11	3	10
12	22	35
13	5	14
14	4	10
15	2	6
16	2	8
17	1	5
18	-1	4

C Change in individual anode currents prior to and after anode change (preheated anodes)

Table 10: Case 10: change in anode currents prior to and after anode change (preheated anodes).

Anode #	Change in mean currents prior to and after anode change [%]	Difference between mean currents prior to and peak currents after anode change [%]
1	17	27
2	4	19
3	-8	24
4	-2	28
5	6	75
6	6	59
7	-74	87
8	-80	15
9	3	50
10	38	121
11	37	139
12	19	140
13	10	96
14	0	99
15	4	64
16	5	69
17	5	71
18	-76	9

Table 11: Case 11: change in anode currents prior to and after anode change (preheated anodes).

Anode #	Change in mean currents prior to and after anode change [%]	Difference between mean currents prior to and peak currents after anode change [%]
1	6	31
2	2	32
3	0	36
4	7	64
5	20	101
6	18	122
7	16	74
8	11	33
9	21	37
10	-3	24
11	4	33
12	-8	91
13	-61	4
14	2	42
15	7	22
16	4	27
17	5	25
18	9	27

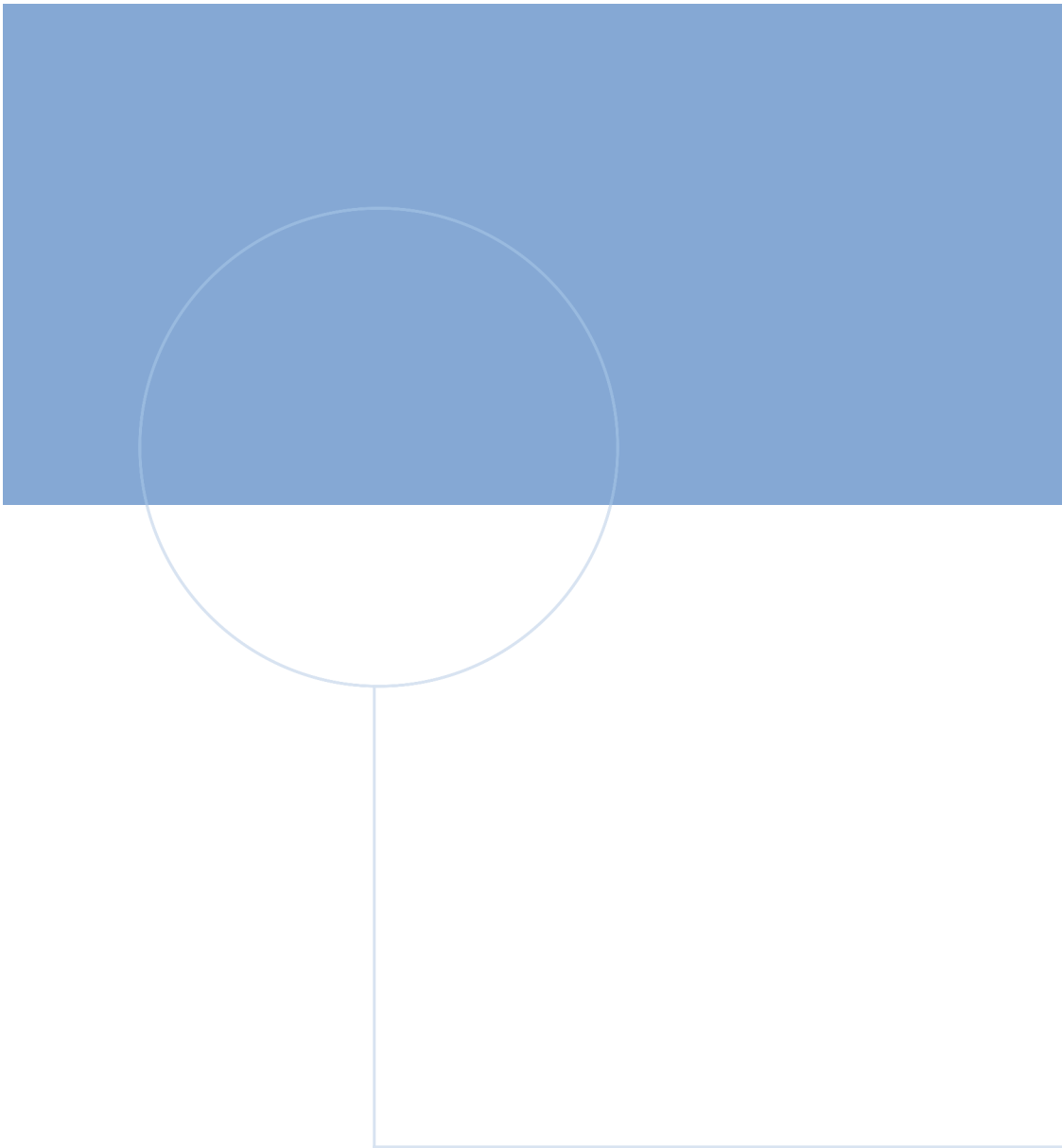

NTNU

Kunnskap for en bedre verden